Lignification mechanism of compression wood cell walls

（圧縮あて材細胞壁の木化メカニズム）

Laboratory of Bio-material Physics

Division of Biological Material Sciences

Department of Biosphere Resources Sciences

Nagoya University

Chikusa-ku Nagoya 464-8601, Japan

Hideto HIRAIDE

September, 2016

Contents

Chapter 1 Introduction

Land plants grow tall and spread their branches to gain efficient photosynthesis; plant stems exhibit negative gravitropism. Plants obtain such tropism during elongation growth. However in woody plant where thickening growth has begun, such tropism cannot occur because elongation growth has finished. Thus they obtained another mechanism to exhibit negative gravitropism during thickening growth (Scurfield 1973, Wilson and Archer 1977). They formed a specialized secondary xylem to generate force called "growth stress", which lift the stem of branches upward (Yamamoto *et al*. 2002).

Woody gymnosperm (soft wood) generates compressive growth stress on the lower side of the inclined stem and branches. The stress is generated in the secondary xylem to push the inclined stem and branches upward (Yamamoto *et al.* 1991, Yamashita *et al*. 2007). Specialized secondary xylem for generation in compressive growth stress is called "compression wood" (Scurfield 1973, Wilson and Archer 1977). On the other hand, woody angiosperm (hard wood) generated tensile stress on the upper side of the inclined stem or branches. Tensile growth stress is generated in the secondary xylem to pull the inclined stem and branches upward. Specialized secondary xylem for generation in tensile growth stress is called "tension wood". Some of angiosperm (*Buxus microphylla*, *Buxus sempervirens*, *Hebe salicifolia*, *Gardenia jasminoides*, *Sarcandra glabra*) form compression-wood-like reaction wood (*Buxus*; Onaka 1949, Bailleres *et al*. 1997, Yoshizawa *et al*. 1993; *Gardenia jasminoides*, Aiso *et al*. 2013; *Sarcandra glabra*, Aiso *et al.* 2014; *Hebe salicifolia*, Kojima *et al*. 2012, planta).

The generation mechanism of the special growth stress was caused by changes in cell wall structure and chemical components (Yamamoto *et al.* 1991, Yamashita *et al*. 2007). In general, tension wood cell wall has lager amount of cellulose content, lower microfibril angle (MFA) than those of normal wood cell. In addition, it includes cellulose rich cell wall with nearly 0 degree of MFA; this special wall termed "G layer". *Magnolia obovata* and Liriodendron tulipifera cell walls have no G layer, but the cell walls have lower MFA and higher cellulose content (Yoshizawa *et al.* 2000, Yoshida *et al.* 2002). Compression wood has higher lignin content than normal wood; and the cell wall is thicker and rich in garactan, and has larger MFA. Lignin concentration is very high in outer portion of the S2 layer; this highly lignified region is termed "S2L" (Timell 1986).

These characteristics of reaction wood show range of intensity (e.g. small-large in growth stress, thin -thick in cell wall, and high-low in lignin content). The case which reaction-wood-specific feature is remarkable represents “severe” reaction wood; the case which reaction-wood-specific feature is tiny represents “mild”. In tension wood, tensile stress is corresponded with the cellulose content, the MFA, and the area rate of G fiber (Okuyama et al. 1990, 1994). In compression wood, compressive stress is corresponded with lignin content and MFA (Yamamoto *et al.* 1991, Yamashita *et al*. 2007). These correspondences suggest combination of the characteristics of reaction wood causes changes in growth stress. Thus anatomical and chemical characteristics of reaction wood are well-studied.

Reaction wood formation is a fundamental mechanism for woody plants. Characteristic in mechanical property, chemical components and cell wall structure have been investigated. Thereafter differentiation process of reaction wood has been investigated, which is necessary to understand overall perspective of reaction wood. To assess this issue, molecular biological approach has been used. Differential display and RNA subtraction methods were used to detect genes that differentially express between normal and reaction woods (Allona *et al*. 1998, Yamashita *et al.* 2009); and these techniques detected genes involved in cell wall formation (e.g. lignin synthesis) and those unpredictable by the anatomical features (calcium transportation, signals transduction). Recently, micro array technique and next generation sequencer (NGS) has been enable us to investigate almost all genes expressed in differentiating normal and reaction woods (Villalobos *et al*. 2012, Sato *et al.* 2014).

Elucidation of the lignin increase mechanism of compression wood is important to understand negative gravitropism in conifers. Because increased lignin in compression wood is believed to lead to compressive growth stress (Boyed 1972, Okuyama *et al.* 1998, Yamamoto *et al.* 1991, Yamashita *et al*. 2007). Additionally, lignin concentration in S2L region has positive correlation with compressive growth stress (Okutama *et al*. 1998).

In the present study, I investigated genes and proteins involved in lignin synthesis. The previous study has reported many genes that differentially express in compression wood from normal wood. However difference in expression level of these genes cannot explain the control of lignin content

among various degrees of compression woods, and the mechanism of S2L formation. Thus, the present study focused on relationship between gene expression level and degree of lignin increase, and localization of the related enzymes. Such advanced study enabled us to discuss the lignin increase mechanism.

In the second chapter, I reported relationship between gene expression involved in lignin synthesis and lignin deposition in differentiation into compression wood of *Chamaecyparis obtusa*. I found a laccase, which can oxidize lignin precursor (monolignol), might function in the compression wood lignification; the laccase gene expressed high in differentiating compression wood while very low in differentiating normal wood; and S2L thickness increased with upregulation the laccase expression level. Peroxidase, which is believed to owed the same stage in lignin synthesis (monolignol oxidization), is also assessed. But the expression level of a peroxidase gene showed no correlation.

I named the compression-wood-specific gene *"CoLac1"* and decided to perform further experiments to reveal the function of this gene.

In the third chapter, I reported *in situ* assays on a laccase encoded by *CoLac1* (CoLac1 laccase). Here, *in situ* means "in the same place the phenomenon is occurring", and in the present study, the *in situ* assays indicate investigating CoLac1 laccase without altering its original localization. We detected localization of laccase activity and CoLac1 laccase in differentiating xylem sections. These assays demonstrated (I) laccase activity is high in the S2L region during secondary wall formation (II) CoLac1 laccase is localized to S2L region, whereas it is less abundant in S1 layer and inner portion of S1 layer. Therefore, I concluded that differentiating cells to compression wood tracheids secrete CoLac1 laccase to S2L region in the onset of S2 formation, which leads to S2L lignification.

In the fourth chapter, we ensured generality of our results by using "compression wood" of *woody angiosperm*. *Buxus microphylla* var. japonica is included in clade of core eudicots, however, it formed closely similar reaction wood to coniferous compression wood. Common mechanism in the formation process between the two might be necessary to form compression wood.

(I) Lignin synthesis genes (PAL and CAD) were upregulated in differentiating reaction wood of

Buxus.

(II) Buxus has a reaction wood specific laccase gene.

(III) In differentiating reaction wood of *Buxus*, laccase activity was higher in S2L region than the other portion.

(IV) Hemicellulose distribution of *Buxus* reaction wood is similar to compression wood of gymnosperm; in the S2L region, garactan is very rich and xylan was decreased compered to normal wood.

Chapter 2

High lignin deposition on the outer region of the secondary wall middle layer in compression wood matches the expression of a laccase gene in *Chamaecyparis obtusa*

Abstract

In compression wood tracheids, the secondary wall middle layer (S2) has a highly lignified region (S2L) in its outer part. To investigate the mechanism of S2L formation and intensification, I assessed the relationship between the expression of genes involved in lignin synthesis and S2L intensity in various degrees of compression wood, from mild to severe. Ultraviolet microscopic analysis of a transverse view of the tracheid cell wall suggested S2L intensification levels. In mild cases, S2L appeared in the parts of S2 close to the cell corner; in moderate cases, the lignin concentration increased and the region expanded, resulting in a connected S2L along a ring; and in severe cases, the ringed S2L thickness increased. qRT-PCR analysis suggested relationships between the expression of genes involved in lignin synthesis and S2L intensification. For monolignol synthesis, expression of eight genes was higher in differentiating compression wood tracheids, but similar among the cases with varying S2L intensities. For monolignol oxidative polymerization, expression of *CoLac1*, encoding laccase, was very high in differentiating compression wood tracheids but very low in differentiating normal wood, and increased in compression wood with increasing S2L thickness. Expression of the other laccase gene (*CoLac2*) was lower in compression wood. Expression of *CoPOX1*, encoding class III plant peroxidase, did not differ between compression wood and normal wood. These results indicate that increased monolignol synthesis enzymes likely do not contribute much to S2L intensification, but that laccase, encoded by *CoLac1*, is likely involved in S2L formation and intensification.

Introduction

The molecular mechanism of S2L formation and intensification would be expected to function in the differentiation into compression wood tracheids. In particular, upregulation of lignin synthesis genes may be involved in S2L formation and intensification. Previous gene expression profiling studies have suggested that levels of laccase, which is involved in the oxidative polymerization of lignin precursors (monolignols), and multiple enzymes involved in monolignol synthesis, increase in differentiating compression wood tracheids versus differentiating normal wood tracheids (Allona *et al.* 1998, Whetten *et al.* 2001, Kotaniemi *et al.* 2007, Yamashita *et al.* 2008, Yamashita *et al.* 2009, Villalobos *et al.* 2012).

Yamashita *et al.* (2009) demonstrated that a laccase gene was upregulated in response to increasing stem inclination angle in *Chamaecyparis obtusa* saplings, and suggested that upregulation of

laccase may have a relationship with increasing lignin abundance. However, it is unclear whether the upregulation of lignin synthesis genes is involved in S2L formation and intensification.

In this chapter, to investigate the contribution of upregulation of lignin synthesis genes to S2L formation and intensification, I assessed relationships between gene expression and S2L intensity. I induced *Chamaecyparis obtusa* saplings to develop compression wood to various degrees by growing them at different inclination angles. In these saplings, I examined S2L intensification in the cell walls of the mature compression wood tracheids and the transcript abundance of lignin synthesis genes in differentiating compression wood tracheids. Based on the results I discuss the contribution of changes in the expression of lignin synthesis genes to S2L formation and intensification.

Materials and Methods

Plant materials

Fifteen Japanese cypress (*Chamaecyparis obtusa*) saplings were used. Twelve were grown with the stem tilted at varying angles to induce compression wood to varying degrees. The angles were 10°, 20°, 30°, and 50° from the vertical; three saplings were used for each angle. The other saplings were grown with the stem vertical (0°) to induce normal wood as controls. One month later (June 13-15, 2011), the saplings were cut down to harvest differentiating and mature tracheids. The differentiating tracheids were shaved off from the stem using a chisel and immediately snap-frozen in liquid nitrogen. The frozen differentiating tracheids were stored at -80°C until RNA extraction. The stem blocks with mature tracheids were harvested from each sapling, and they were then fixed in 3% glutaraldehyde in 0.1 M phosphate buffer (pH 6.98) and were embedded in epoxy resin for ultraviolet microscopic analysis.

Ultraviolet microscopic analysis

To investigate the lignin distribution in compression and normal wood tracheids, ultraviolet microscopy was performed. Transverse sections (1 μm thick) were prepared using an ultramicrotome (MICROM HM350, Carl Zeiss, Germany). The sections were mounted on quartz slides, immersed in a drop of glycerol, and covered with a quartz coverglass. Ultraviolet photomicrographs were taken at a wavelength of 280 nm using ultraviolet microscopic spectrophotometers (MPM800, Carl Zeiss, Germany) equipped with an ultraviolet-sensitive CCD camera (CM-140 GE-UV, JAI, Denmark). The image data of the ultraviolet photomicrographs with 256 gradations were analyzed using the ImageJ software (http://rsb.info.nih.gov/ij/). The darkness of images increased as the absorption of lignin in the cell wall increased, although the relationship between darkness and absorption may not be strictly proportional. In this study, we defined the specific region in the outer S2 where the lignin concentration was higher than in

the inner part of S2 as "S2L." To estimate the average thickness of S2L in a compression wood cell wall, the area of the perimeter and lumen side of S2L were measured in each tracheid using ImageJ. Using circles with the same area as the measured figures, I defined the difference between the radii of the two circles as the average thickness of S2L. Thirty tracheids were analyzed for each sapling. To assess the lignin concentration of S2L semi-quantitatively, I use the darkness of image data with 256 gradations as 280-nm absorption darkness (arbitrary units = 0-255). The 280-nm absorption darkness profiles along the line through a double cell wall were used to compare the S2L lignin concentrations among saplings.

cDNA cloning

To profile the transcripts expressed in differentiating tracheids, the cDNA sequences were determined. Total RNA was extracted from differentiating tracheids using the same method as described for the quantitative reverse transcription polymerase chain reaction (qRT-PCR). cDNA was synthesized from total RNA using the PrimeScript RT-PCR kit (TaKaRa, Japan). To amplify cDNAs for genes involved in lignin synthesis, degenerate primer pairs or mixed oligonucleotide primer pairs were used. The degenerate primer pair for POX was designed by Marjamaara *et al.* (2006). The degenerate primer pairs for each gene were designed corresponding to the conserved amino acid sequence of land plant species. Mixed oligonucleotide primer pairs were designed corresponding to the nucleotide sequences conserved in coniferous species. The sequences of degenerate/mixed oligonucleotide primers are shown with the amino acid sequence used in Table 1. The reaction mixture for PCR amplification consisted of cDNA from differentiating tracheids, 2-μL 10×Ex Taq Buffer, 0.4 mM dNTP mixture, 0.5 units TaKaRa Ex Taq HS, and 5 μM sense and antisense primer in a total volume of 20 μL. The amplified cDNA fragments were inserted into the pGEM-T Easy Vector (Promega, USA) and their sequences were determined. A partial transcript sequence of the laccase gene of *Chamaecyparis obtusa* (AB361315), termed *CoLac1* in this study, was obtained from the DNA Data Bank of Japan. To estimate proteins encoded by the transcript sequences obtained, similarity searches of genes in the *Arabidopsis thaliana* genome were performed using BLAST X of TAIR (http://www.arabidopsis.org/). The new sequences were submitted to the DNA Data Bank of Japan.

Rapid amplification of cDNA ends (RACE)

To obtain full-length transcript sequences of laccases and the POX gene (*CoLac1*, *CoLac2*, *CoPOX1*), I performed 3' and 5' rapid amplification of cDNA ends (RACE). cDNA fragments including 3' and 5' ends were obtained with the SMARTer RACE cDNA Amplification kit (Clontech, USA). Total RNA was extracted from differentiating tracheids according to the method described for qRT-PCR. 3'

RACE-Ready cDNA and 5’ RACE-Ready cDNA were synthesized in a volume of 10 μL with 1-μg total RNA according to the manufacturer’s protocols, followed by the addition of 100-μL Tricine-EDTA buffer to dilute the solution. Both gene-specific sense primers for 3’ RACE and gene-specific antisense primers for 5’ RACE were designed corresponding to the transcript sequences. The primer sequences were as follows: 3’ RACE for *CoPOX1*, ATGGG ACATC AAGCG AAAGG GTGGC TC; 5’ RACE for *CoPOX1*, GTGGG CGCGG GTATA CTGTC ATCAA CAG; 5’ RACE for *CoLac1*, GAATG AGGAA TGTGG CATTG GGTGG CTG; 3’ RACE for *CoLac2*, CGTAA TCTGT TCTTC GCAAT GGGGC TTG, 5’ RACE for *CoLac2*, TGTGT GATGT ATGCA GGCCC ATCAG C.

3’ RACE-PCR was performed in a 20-μL volume with 1-μL 3’ RACE-Ready cDNA, 0.2 μM gene-specific sense primer, 2-μL 10× universal primer mix, and 0.4-μL 50× Advantage 2 polymerase mix (Clonetech, USA). The reaction conditions were as follows: *CoLac2* (94°C for 30 s, 72°C for 90 s) × 5, (94°C for 30 s, 70°C for 30 s, 72°C for 90 s) × 5, (94°C for 30 s, 68°C for 30 s, 72°C for 90 s) × 35, and 70°C for 10 min, and *CoPOX1* (94°C for 30 s, 72°C for 60 s) × 5, (94°C for 30 s, 70°C for 30 s, 72°C for 60 s) × 5, (94°C for 30 s, 68°C for 30 s, 72°C for 60 s) × 30, and 70°C for 10 min.

5’ RACE-PCR was performed in a 20-μL volume with 1-μL 5’ RACE-Ready cDNA, 0.2 μM gene-specific antisense primer, 2-μL 10× universal primer mix, and 0.4-μL 50× Advantage 2 polymerase mix (Clonetech, USA). The reaction conditions were as follows: *CoLac1* (94°C for 30 s, 72°C for 60 s) × 5, (94°C for 30 s, 70°C for 30 s, 72°C for 60 s) × 5, (94°C for 30 s, 68°C for 30 s, 72°C for 60 s) × 25, and 70°C for 10 min, and *CoLac2* (94°C for 30 s, 72°C for 90 s) × 5, (94°C for 30 s, 70°C for 30 s, 72°C for 90 s) × 5, (94°C for 30 s, 68°C for 30 s, 72°C for 90 s) × 40, and 70°C for 10 min, and *CoPOX1* (94°C for 30 s, 72°C for 60 s) × 5, (94°C for 30 s, 70°C for 30 s, 72°C for 60 s) × 5, (94°C for 30 s, 68°C for 30 s, 72°C for 60 s) × 30, and 70°C for 10 min.

Because the 5’ RACE-PCR product of the POX gene (*CoPOX1*) included several extra fragments, 5’ nested RACE-PCR was performed to generate a single fragment. The gene-specific antisense primer sequence for the nested 5’RACE for *CoPOX1* was CGATA GAATG GTCCT CCGGC CTTGT TG. The reaction was performed in a 20-μL volume with 2-μL 5’ RACE-PCR product diluted 1:50 with Tricine-EDTA Buffer, 0.2 μM gene-specific antisense primer, 2-μL 10× universal primer mix, and 0.4-μL 50× Advantage 2 polymerase mix (Clonetech). The reaction conditions were as follows: (94°C for 30 s, 68°C for 60 s, 72°C for 60s) × 15, and 70°C for 10 min.

The 3’ and 5’ RACE-PCR products were inserted into the pGEM-T Easy Vector (Promega, USA) and sequenced.

Construction of a phylogenetic tree

To estimate the functions of the laccases encoded by *CoLac1* and *CoLac2*, I constructed a phylogenetic tree composed of laccases from both gymnosperms and angiosperms using the Clustal W service of the DDBJ (http://clustalw.ddbj.nig.ac.jp/index.php?lang=ja), where *Coriolus versicolor* laccase was used as the outgroup. The amino acid sequences from *Pinus taeda*, *Populus trichocarpa*, *Oryza sativa*, *Acer pseudoplatus*, and *Coriolus versicolor* were obtained from NCBI (http://www.ncbi.nlm.nih.gov/). The amino acid sequences from *Arabidopsis thaliana* were obtained from TAIR (http://www.arabidopsis.org/). The accession numbers for laccase genes from the other species were as follows: *Populus3*, *90*, *110* (y13771, y13772, y13773), *Pinus1-8* (AF132119-AF132126), *Oryza1*, *3-7* (AF047697, BAB92845, BAB92843, BAB90733, BAB86465, BAB86452), *Acer1* (U12757), and *Coriolus versicolor* (D13372). The loci of laccase genes in the *Arabidopsis thaliana* genome were as follows: *AtLac1-17* (AT1G18140, AT2G29130, AT2G30210, AT2G38080, AT2G40370, AT2G46570, AT3G09220, AT5G01040, AT5G01050, AT5G01190, AT5G03260, AT5G05390, AT5G07130, AT5G09360, AT5G48100, AT5G58910, AT5G60020). The multiple amino acid sequence alignment was used to construct a neighbor-joining tree (1,000 bootstraps). The tree was presented using TreeView (Page 1996).

qRT-PCR

To investigate transcript abundance in differentiating normal wood and compression wood tracheids, I performed qRT-PCR analysis. Total RNAs were extracted from 50-mg differentiating tracheids using the RNeasy Plant Mini Kit (QIAGEN, Germany) according to the manufacturer's protocols and treated with DNase I (TaKaRa, Japan) to remove contaminating genomic DNA. Absence of contaminating genomic DNA was confirmed by an absence of PCR amplification of the cyclophilin gene (a reference gene for qRT-PCR analysis). The RNA concentration was estimated spectrophotometrically using Gene Quant (Amersham, Germany). The cDNAs were synthesized at 37°C for 30 min with 500-ng total RNA in a volume of 15 μL using PrimeScript RT Master Mix (Perfect Real Time; TaKaRa, Japan); the cDNAs were then diluted 3:10 with water.

Gene-specific primers were designed using Primer 3 Plus (http://www.bioinformatics.nl/cgi-bin/primer3plus/primer3plus.cgi) and the sequences shown in Table 2. The amplification was performed in triplicate using the StepOnePlus Real Time PCR System (Applied Biosystems, USA). The baseline and the threshold cycle were determined automatically using the StepOne software ver. 2.1 (Applied Biosystems, USA). The 20-μL reaction mixture consisted of 0.5-μL cDNA, 200 nM sense and antisense primers, and 10-μL POWER SYBR Green PCR Master Mix (Applied Biosystems, USA). The reaction conditions were as follows: 95°C for 10 min (95°C for 15 s, 58°C for 60 s) × 40. To assess possible extra products, after the melting curve was analyzed, I performed agarose gel

electrophoresis analysis and confirmed the absence of additional bands.

The absolute number of transcripts was determined from a standard curve, obtained from serial dilutions of linear plasmids containing the target sequence. Except for the 18SrRNA gene (one of the reference genes for qRT-PCR analysis), the standard curves from 1:10 serial dilution spanned a range of 250 to 2,500,000 copies of the target sequence. For the 18SrRNA gene, the standard curve spanned 25,000 to 250,000,000 copies. To prepare linear plasmids, PCR products, including a target sequence, were inserted into the pGEM-T Easy Vector (Promega, USA). The plasmids were linearized with Sac II and then purified with phenol:chloroform:isoamyl alcohol (25:24:1, v/v). The molar concentrations were determined spectrophotometrically using Gene Quant (Amersham, Germany). To confirm the accuracy of the determination, agarose gel electrophoresis was performed, and I confirmed that the linear plasmids were identical in intensity with the same amount of λ-*Bst*P I (TaKaRa, Japan) fragment.

To estimate transcript abundance accurately, I used the normalization method proposed by Vandesompele *et al*. (2002). According to this method, transcript abundance represents the ratio of the transcript number of target gene to the normalization factor (NF), where NF is the geometric mean of transcript numbers of proper reference genes. As appropriate reference genes to obtain NF, I selected cyclophilin (AB505627), eukaryotic translation initiation factor SUI1 (AB762664), 18SrRNA (EF673741), and polyubiqutin (BW987637).

Results

Lignin distribution in tracheid cell walls with varying degrees of compression wood

I induced saplings to produce tracheids in stems with various degrees of compression wood. To investigate S2L intensification in mature compression wood tracheids, I observed lignin distribution in the cell wall using an ultraviolet microscope at a wavelength of 280 nm (Figure 1a). Because lignin absorbs ultraviolet rays at 280 nm, the more highly lignified regions appear darker (Fergus *et al*. 1969, Yoshida *et al*. 2002). Normal wood tracheids were observed in the vertical saplings. In the secondary walls, the lignin concentration was uniform and no S2L was observed. In contrast, compression wood tracheids were observed in all of the tilted saplings. In the compression wood tracheids, S2L was observed, and varied in thickness. In the compression wood tracheids with thin S2L, the lignin concentration in the whole region of the secondary wall was higher than in the normal wood tracheids, and S2L appeared close to the cell corners rather than along the ring. In cases with a thick S2L, the lignin concentration in the whole region of the secondary wall was higher than in the presence of thin S2L, and S2L was formed along the ring. In cases with a very thick S2L, the lignin concentrations in S2L and the inner region of S2 were similar to those in cases with a “thick S2L.”

The thickness of S2L in transverse view was 0.48-1.65 μm in tilted saplings; mean thicknesses differed among saplings (Figure 1b). The lignin concentration (280-nm absorption darkness) of S2L in tilted saplings (compression wood) was higher than that of S2 in vertical saplings (normal wood; Figure 1c). Additionally, the lignin concentrations of S2L were similar among the saplings with thick to very thick S2L (Fig.1c).

cDNA cloning

In coniferous species, lignin in the secondary xylem, including compression wood, is composed principally of guaiacyl units, with few p-hydroxy units (Adler 1977, Nimz *et al* 1981); these units are derived from coniferyl and p-coumaryl alcohol, respectively. Two types of monolignols are synthesized from L-phenylalanine by eight enzymes: phenylalanine ammonia-lyase (PAL), p-coumarate 3-hydroxylase (C3H), cinnamate-4-roxylase (C4H), 4-coumarate:CoA ligase (4CL), hydroxycinnamoyl-CoA shikimate/quinate hydroxycinnamoyl transferase (HCT), caffeoyl-CoA O-methyltransferase (CCoAOMT), cinnamoyl CoA reductase (CCR), and cinnamyl alcohol dehydrogenase (CAD) (Boejan *et al* 2003). The oxidative polymerization of monolignols for lignin deposition is catalyzed by laccase (Lac) or class III plant peroxidase (POX) (Vanholme *et al*. 2010).

To profile lignin synthesis gene transcripts, partial cDNA sequences were determined. Additionally, full-length cDNA sequences for POX and laccase were determined using the RACE method. I assessed the similarities of the partial and full-length cDNA sequences to the *Arabidopsis thaliana* genome sequence using TAIR BLAST searches (Table 3). All of the cDNA sequences showed high identities to lignin synthesis genes (e-value < 10^{-5}). For monolignol synthesis, two genes encoding PAL (*CoPAL1* and *CoPAL2*) and a single gene encoding each of the other enzymes (*CoC3H1*, *CoC4H1*, *CoHCT1*, *CoCCoAOMT1*, *CoCCR1*, and *CoCAD1*) were cloned. For oxidative polymerization of monolignols, the genes encoding POX and laccase were cloned. The cloned sequences are available under the following accession numbers: *CoPAL1* (AB762652), *CoPAL2* (AB762653), *CoC4H1* (AB762654), *Co4CL1* (AB762655), *CoC3H1* (AB762656), *CoHCT1* (AB762657), *CoCCoAOMT1* (AB762658), *CoCCR1* (AB762659), *CoCAD1* (AB762660), *CoPOX1* (AB762661), *CoLac1* (AB762662), and *CoLac2* (AB762663).

Phylogeny of laccase genes

To estimate the possible functions of the two laccases from *C. obtusa* (*CoLac1* and *CoLac2*), I constructed a phylogenic tree composed of *CoLac1*, *CoLac2*, and known laccase genes from gymnosperms and angiosperms (Figure 2). The tree formed three clusters, consisting of both gymnosperms and

angiosperms (G1, G2, and G3). *CoLac1* was included in G1 with *Populus110* (Y13773), *Pinus1, 3, 5, 6* (AF132119, AF132121, AF132123, AF132124), *Oryza1, 6, 7* (AF047697, BAB86465, BAB86452), and *AtLac2, 17*.*CoLac2* was included in G2 with *Pinus7, 8* (AF13211, AF13212), *Populus3* (Y13771), *Oryza5* (BAB92843), and *AtLac4, 10, 11, 16* (AT2G38080, AT5G01190, AT5G03260, AT5G58910).

Relationship between S2L thickness and gene expression

To investigate the relationship between the S2L thickness and the expression of genes involved in lignin synthesis, I performed gene expression analyses in differentiating compression wood tracheids by qRT-PCR (Figure 3). The transcript abundance of most of monolignol synthesis genes (*CoPAL1*, *CoPAL2*, *CoC4H1*, *CoC3H1*, *CoHCT1*, *CoCCoAOMT1*, *CoCCR1*, and *CoCAD1*), each of which encodes an enzyme in the monolignol synthesis pathway, was higher in compression wood than in normal wood (Figure 3a-i). The transcript abundances of these monolignol synthesis genes were similar among saplings with various thicknesses of S2L. The transcript abundance of *CoPOX1*, encoding POX, showed no obvious pattern between compression wood and normal wood samples (Figure 3j). The transcript abundance of *CoLac1*, encoding laccase, was very high in compression wood while very low in normal wood, and was higher in the saplings with thicker S2L (Figure 3k). The transcript abundance of *CoLac2*, also encoding a laccase, was lower in compression wood, and did not differ among saplings with various S2L thicknesses (Figure 3l). *CoLac2* transcript abundance was also much lower than that of *CoLac1* in differentiating compression wood (Figure 3k and l; compare the vertical axes).

Discussion

S2L intensification in compression wood tracheids

Ultraviolet microscopic analysis of the tracheid cell walls with varying degrees of compression wood showed S2L intensification (Figure 1a). In mild cases, S2L appeared in the parts of S2 close to the cell corner; in moderate cases, the lignin concentration increased and the region expanded, resulting in a connected S2L along a ring; and in severe cases, the ringed S2L thickness increased. Lignin concentrations in S2L were similar among saplings with thick to very thick S2L (Figure 1c). This result suggests that S2L thickness increases after the lignin concentrations in S2L reach a peak.

Several studies have suggested that lignin deposition in S2 generates compressive growth stress, together with an increase in microfibril angle (Okuyama *et al*. 1998, Yamamoto *et al*. 1998). Thus, *Chamaecyparis obtusa* may enhance compressive growth stress by not only lignifying S2L but also thickening S2L in compression wood tracheids.

Possible function of the two laccases (*CoLac1* and *CoLac2*) during differentiation into compression wood tracheids

Several laccases from land plant species catalyze the oxidization of a broad range of phenol substrates in addition to monolignol *in vitro* (Sterjiades etal. 1998, Bao *et al*. 1993, Ranocha *et al*. 1999). Their potential physiological/biochemical functions are also believed to be diverse. One of their main functions is oxidizing monolignols in lignin synthesis. To assess whether the two laccases (*CoLac1* and *CoLac2*) encoded in the *C. obtusa* genome were involved in monolignol oxidative polymerization, I constructed a phylogenic tree composed of *CoLac1*, *CoLac2*, and other laccase genes from gymnosperms and angiosperms (Figure 2).

The phylogenetic tree showed three clusters, consisting of both gymnosperms and angiosperms (G1, G2, and G3; Figure 2). *CoLac1* was included in G1, together with *AtLac17* and *Populus110*. This result suggested that *CoLac1* may be orthologous to these laccase genes, and the laccase encoded by *CoLac1* may have a similar function to those laccase genes. A study of an *AtLac17*-knockdown mutant of *Arabidopsis thaliana* demonstrated that *AtLac17* was involved in the deposition of guaiacyl units of lignin polymers in interfascicular fibers (Berthet *et al*. 2011). Additionally, laccase encoded by *Populus110* of *Populus euramericana* is expressed in differentiating secondary xylem, and catalyzes the oxidization of coniferyl alcohols (precursors of guaiacyl lignin) *in vitro* (Ranocha *et al*. 1999). Therefore, it seems reasonable that the laccase encoded by *CoLac1* likely oxidizes monolignols for lignin deposition.

CoLac2 was included in G2 together with *Pinus7*, *Pinus8*, *AtLac4*, and *AtLac11*. This suggested that *CoLac2* is most closely related to *Pinus7* and *Pinus8* among *Pinus* laccase genes and orthologous to *AtLac4* and *AtLac11*. *Pinus7* and *Pinus8* are most highly expressed in immature secondary xylem, compared with other tissues, such as phloem, needles, shoot tips, immature pollen cones, and roots (Sato *et al*. 2001). A study of the *AtLac4*-knockout and -knockdown mutants demonstrated that *AtLac4* is involved in lignin deposition in vascular bundles and interfascicular fibers (Berthet *et al*. 2011). *AtLac11* is also involved in lignin deposition in the stem with *AtLac4 and AtLac17* (Zhao *et al*. 2013). Therefore, it seems reasonable that the laccase encoded by *CoLac2* likely oxidizes monolignols for lignin deposition.

Contribution of the upregulation of lignin synthesis genes to S2L formation and intensification

All of the cDNA sequences cloned from differentiating tracheids of *Chamaecyparis obtusa* showed high similarity to the lignin synthesis genes of the *Arabidopsis thaliana* genome (Table 3). This result suggests that the transcripts cloned from differentiating tracheid encode lignin synthesis enzymes. The transcript sequences enabled us to investigate the transcript abundance in differentiating tracheid by qRT-PCR.

The expression of monolignol synthesis genes was higher in compression wood than in normal wood (Figure 3 a-i). To assess the significance of differences in transcript abundance from normal wood (group of three vertical saplings), I performed Student's or Welch's t-test for each gene (if equal variance, Student's t-test was used, and if unequal variance, Welch's t-test was used). The transcript abundances of *CoPAL1*, *CoPAL2*, *CoC3H1*, *CoC4H1*, *CoHCT1*, *CoCCoAOMT1*, *CoCCR1*, and *CoCAD1* were statistically significantly higher in compression wood (group of 12 tilted saplings; $P < 0.05$). Similar results were reported in other coniferous species (Allona *et al*. 1998, Whetten *et al*. 2001, Kotaniemi *et al.* 2007, Yamashita *et al*. 2008, Yamashita *et al*. 2009, Villalobos *et al.* 2012). Thus, additional monolignols may be supplied to increase lignin abundance in the tracheid, or to form S2L in the cell wall. However, such upregulation of monolignol synthesis genes showed no obvious relationship with S2L intensification. This result indicates that the increased expression of monolignol synthesis enzymes apparently did not contribute much to S2L intensification. Thus, S2L intensification may require other factors beyond simply an increase in monolignol supply. For example, the hemicellulose distribution in the cell wall, which is believed to provide appropriate conditions for lignin deposition (Terashima eta al. 1989, Terashima eta al. 1993), and enzymes catalyzing monolignol oxidative polymerization, may also be involved in S2L intensification, because compression wood tracheids have different hemicellulose distributions than normal wood (Kim *et al*. 2010, Donaldson and Knox 2012) and a laccase gene (*CoLac1*) was upregulated in differentiation into compression wood tracheids in this study (Figure 3k).

CoPOX1 expression showed no specific pattern between compression and normal wood (Figure 3j). *CoPOX1* expression seemed not to change during differentiation into compression wood. This suggests that changes in the expression of *CoPOX1* are not essential for differentiation into compression wood tracheids. Several POX genes that were upregulated in differentiating xylem in compression wood were reported in a previous study that used qRT-PCR analysis with ESTs of *Picea abies* (Koutaniemi *et al*. 2007). However, no POX gene upregulated in the differentiating xylem of compression wood was detected in previous microarray analyses of cDNAs and ESTs of *Pinus taeda* Whetten *et al*. 2001) and *Pinus pinaster* Ait (Villalobos *et al*, 2012). Additionally, a study of a laccase triple mutant of *Arabidopsis thaliana* (simultaneous disruption of *AtLac11*, *AtLac4*, and *AtLac17*) suggested that lignin deposition in the stems, which is the homologous organ to coniferous stems, involved not POXs but laccases (Zhao *et al*. 2013). Thus, whether POXs are involved in monolignol oxidative polymerization during differentiation into compression wood tracheids warrants further investigation.

The expression of *CoLac1* was very low in differentiating normal wood and very high in differentiating compression wood: S2L was formed when *CoLac1* was expressed, and vice versa (Figure 3k). This result suggests that *CoLac1* is involved in S2L formation and that *CoLac1* may be a specialized

gene for differentiation into compression wood tracheids. Several studies have reported that the genes encoding laccase or laccase-type polyphenol oxidases are more abundant in differentiating xylem in compression wood in other coniferous species, such as *Pinus taeda* Allona *et al*. 1998), *Picea abies* (Koutaniemi *et al*. 2007), and *Picea sitchensis* (McDougall 2000). Thus, the specific function of laccase in S2L formation is likely conserved in many coniferous species. Moreover, the expression of this compression-wood-special laccase gene of *Chamaecyparis obtusa* increased with S2L thickening (Figure 3k). To investigate the correlation of transcript abundance with S2L thickness, I used Pearson's correlation coefficient test in the compression wood group (12 tilted saplings) to assess the correlation between the 12 transcript abundance levels and 360 measurements of S2L thickness. The *CoLac1* transcript abundance showed a positive correlation with S2L thickness ($P < 0.01$, $R = 0.585$). These results suggest that upregulation of *CoLac1* was involved in the intensification of S2L.

The expression of *CoLac2* in differentiating compression wood tracheids was considerably lower than that of *CoLac1* (Figure 3k and l; compare the vertical axes). This result suggests that monolignol oxidative polymerization during differentiation into compression wood tracheids is catalyzed by the laccase encoded by *CoLac1* than that encoded by *CoLac2*. The expression of *CoLac2* was stable in differentiating normal wood tracheids, but lower in differentiating compression wood tracheids (Figure 3l). This result suggests that *CoLac2* is downregulated during differentiation into compression wood tracheids. Thus, the encoded laccase may be involved in lignin deposition during differentiation into normal wood tracheids.

Table 1. Sequences of degenerate/mixed oligonucleotide primer pairs for cDNA amplification.

Target enzyme	Sense primer sequence (amino acid sequence), Antisense primer sequence (amino acid sequence): Primer sequence 5'→3'	Expected product size
Phenylalanine ammonia-lyase (PAL)	GCN GAR CAR CAY AAY CAR GAY GT (AEQHNQDY), TA IAR IGG RTA ISI NCK RCA YTC (ECRSYPLY)	550 bp
Cinnamate-4-hydroxylase (C4H)	AAR GGN CAR GAY ATG GT (KGQDMV), AC RTT RTC YTC RTT DAT YTC (EINEDNV)	560 bp
4-Coumarate:CoA ligase (4CL)	CAR CAR GTN GAY GGN GA (QQVDGE/D), GG NGC NAC YTG RAA NCC YTT (KGFQVAP)	720 bp
Coumarate 3-hydroxylase (C3H)	ATH TGG GCN GAY TAY GG (IWADYG), GC NGT DAT CAT RTC CCA (WDMITA)	570 bp
Hydroxycinnamoyl-CoA shikimate/quinate hydroxycinnamoyl transferase (HCT)	GTN CCN TTY TAY CCN ATG (VPFYPM), AT NAC RTT NCC RAA RTA NCC (GYFGNVI)	720 bp
Caffeoyl-CoA O-methyltransferase (CCoAOMT)	GCN AAR CAY CCN TGG AA (AKHPWN), AA RTC DAT YTT RTG NGC NAC (VAHKIDF)	250 bp
Cinnamoyl CoA reductase (CCR)	GTN TGY GTN ACN GGN GC (VCVTGA), TT NCC RTA RCA RTA CCA RT (NWYCYGK)	460 bp
Cinnamyl alcohol dehydrogenase (CAD)	GTI CCI GGN CAY GGN GTN GT (VPGHGVV), AC NCC CAT RTG NCC NAC NCC (GVGHMGV)	390 bp
Class III plant peroxidase (POX)	CTICAYTTYCAYGAR TGC, GTRTGISCICCNGATAGGGC NC	400 bp
Laccase (Lac)	AGGSWRAAACSAGRCATTA, GTGAASACRCCRCTGATGT	1100–1200 bp

W, A+T; R, A+G; M, A+C; K, T+G; Y, C+T; S, C+G; D, A+T+G; H, A+T+C; B, T+C+G; V, A+C+G; N, A+C+G+T; I, Deoxyinosine.

Table 2. Sequences of the gene-specific primer pairs for qRT-PCR.

Target gene	Sense primer sequence, Antisense primer sequence: Primer sequence 5'→3'	Product size
CoPAL1	GCGCTGGGTATTCTCTGATG, CCCTTGTCATAACTAGCCCTTG	181 bp
CoPAL2	TGCCTCATACCCTCTCTTCC, TGTCAACCTCAACTGGTAGGC	155 bp
CoC4H1	GGCTTTGAATGGTGAAAGGA, TGGGGATGAAATCTCCGTAA	68 bp
Co4CL1	ATCGACACAGAGACCGGAGT, AATTTCAGGTCCACGAATGC	72 bp
CoC3H1	TTCCCTATCTCCGTTGGATG, TGTTTGGCACCACTCTTCTG	130 bp
CoHCT1	TGGCCTACAGCAGCTATGAA, TCTGCCATCTGTTGCAATGT	113 bp
CoCCoAOMT1	TGACTACTTCGGCTGATGAGG, CCATGGTGTTCTTGGCATTA	72 bp
CoCCR1	GCACATCTGAAACAGCTGGA, CAGGCTCCACCATTTGAACT	160 bp
CoCAD1	ATTGGAGAGCATGTGGGTGT, AGCAAATCCTCCTTGTGTGG	150 bp
CoPOX1	GGTTGCTCTTTCAGGTGGAC, TGGTCGAGAGTGGGATCTTC	111 bp
CoLac1	ATCCTTCATTCAACCCACCA, AGGGTCCGTGTGTTGTTAGG	141 bp
CoLac2	TCCAATCCCATAATGCCTGT, CCCATTGCGAAGAACAGATT	146 bp
Cyclophilin	TGAGTCCATTTACGGTGCAA, AGAACTGGGAGCCATTGGTA	113 bp
Eukaryotic translation initiation factor SUI1	ATTTGATCCATTCGCTGAGG, CTTTCTACCGTTTCGCTGTTG	94 bp
Polyubiquitin	TCATTTGCAGGTTCTGTGTTG, CTTTGCCTTCACATTGTCGAT	129 bp
18SrRNA	AGTCTGGTCCTGTTCCGTTG, CTTTCGCAGTGGTTCGTCTT	125 bp

Table 3. Similarities of the cDNA sequences to the *Arabidopsis thaliana* genome.

Gene name	Length of cloned coding region (bp)	Locus of the most homologous gene in the *Arabidopsis thaliana* genome	Locus description	e-value	Amino acid identity
CoPAL1	490	AT2G37040	Phenylalanine ammonia-lyase (PAL1)	1e-51	60%
CoPAL2	490	AT2G37040	Phenylalanine ammonia-lyase (PAL1)	6e-60	66%
CoC4H1	517	AT2G30490	Cinnamate-4-hydroxylase	8e-71	72%
Co4CL1	676	AT1G51680	4-Coumarate:CoA ligase (4CL1)	4e-97	75%
CoC3H1	517	AT2G40890	Coumarate 3-hydroxylase (CYP98A3)	1e-72	77%
CoHCT1	675	AT5G48930	Hydroxycinnamoyl-Coenzyme A shikimate/quinate hydroxycinnamoyltransferase	9e-93	69%
CoCCoAOMT1	221	AT4G34050	Caffeoyl-CoA O-methyltransferase (CCoAOMT1)	1e-23	73%
CoCCR1	422	AT1G15950	Cinnamoyl CoA reductase	9e-60	76%
CoCAD1	355	AT3G19450	Cinnamyl alcohol dehydrogenase (CAD4)	5e-45	66%
CoPOX1	1059	AT1G71695	Peroxidase	2e-97	50%
CoLac1	1743	AT5G60020	Laccase (laccase 17)	0.0	62%
CoLac2	1665	AT5G03260	Putative laccase (laccase 11)	0.0	64%

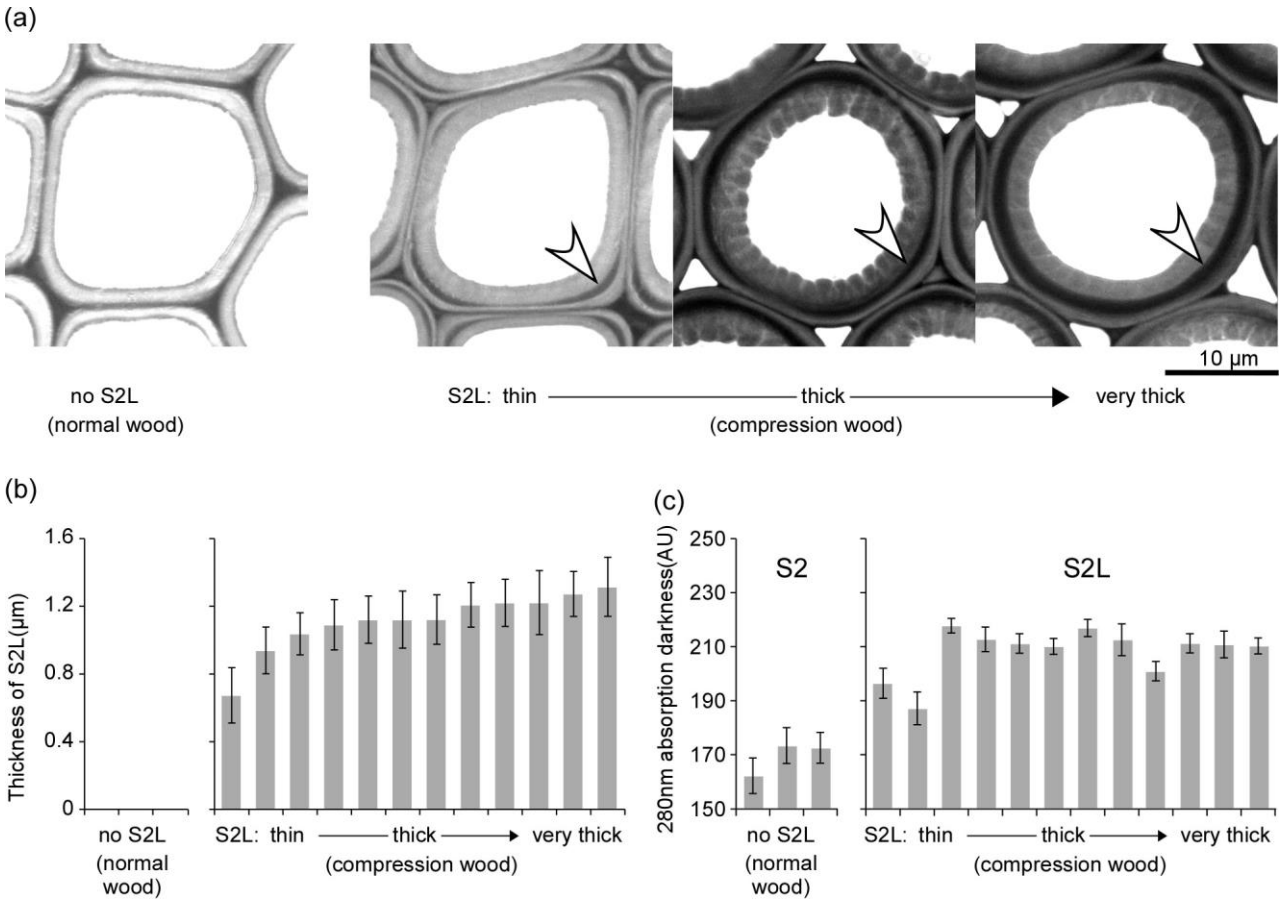

Figure 1. Lignin distribution in tracheid cell walls with varying degrees of compression wood.

(a) Lignin distribution in a transverse view of tracheid cell walls by ultraviolet microscopy. The photograph on the left is a normal wood tracheid from a vertical sapling. The photographs on the right are compression wood tracheids from tilted saplings with varying S2L thicknesses. The arrowhead indicates S2L.

(b) Thickness of S2L in each tilted sapling. Values are means ± SD of 30 tracheids. In the vertical sapling (normal wood), no S2L was observed.

(c) S2L 280-nm absorption darkness in a tilted sapling. Values are means ± SD of 30 measurements, derived from 15 double cell walls. For a vertical sapling (normal wood), the 280-nm absorption darkness of S2, is shown as a control.

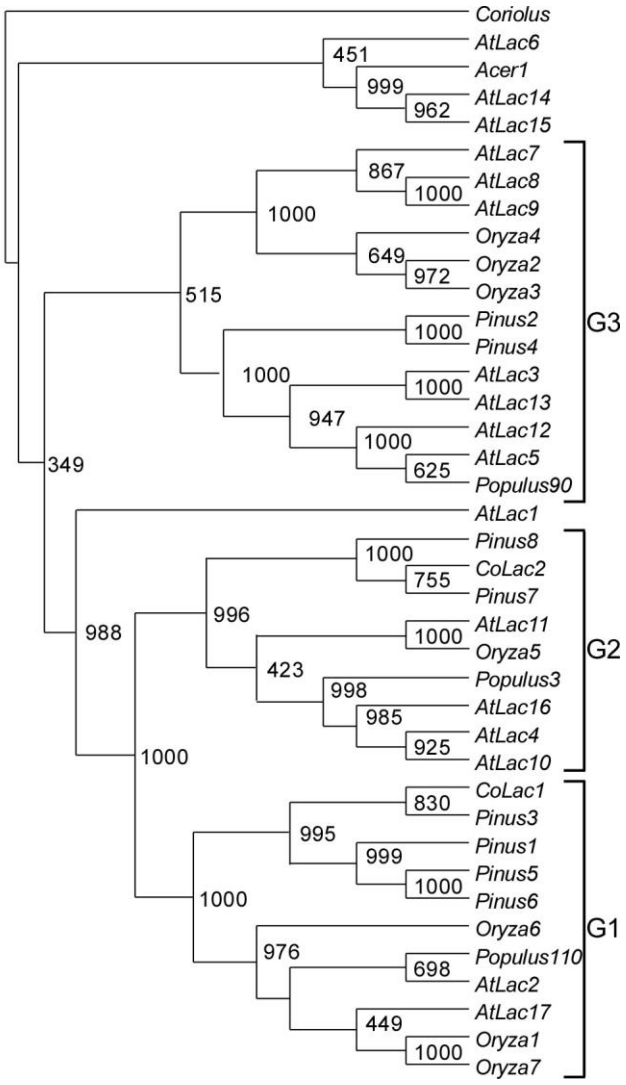

Figure 2. Phylogenetic tree composed of *CoLac1*, *CoLac2*, and known laccase genes from gymnosperms and angiosperms. The tree was constructed with multiple amino acid alignments using ClustalW. *Coriolus versicolor* laccase was used as the outgroup. Numbers in nodes indicate bootstrap support for each group from 1,000 pseudoreplicates. The tree formed three clusters consisting of both gymnosperms and angiosperms (G1, G2, and G3).

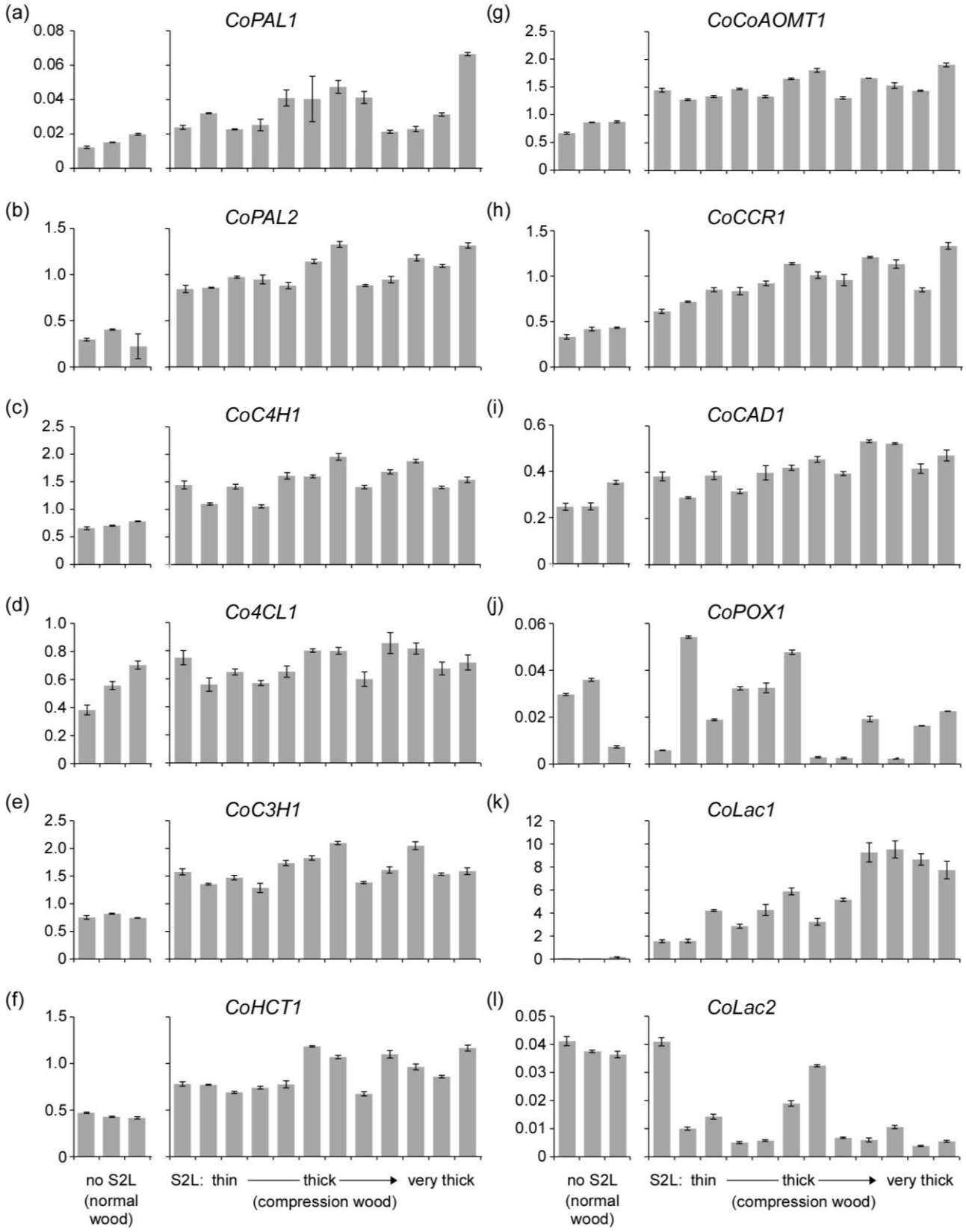

Figure 3. Transcript abundance of lignin synthesis genes in tilted saplings developing compression wood tracheids with varying S2L thicknesses. a) *CoPAL1*, b) *CoPAL2*, c) *CoC4H1*, d) *Co4CL1*, e) *CoC3H1*, f)

CoHCT1 g) *CoCCoAOMT1*, h) *CoCCR1*, i) *CoCAD1*, j) *CoPOX1*, k) *CoLac1*, and l) *CoLac2*. Vertical axis indicates transcript abundance, representing the ratio of the transcript number of the target gene to NF. Values are means ± SD of three independent measurements for each sapling. Note that the vertical axis scales differ among the genes examined. Transcript abundance in the vertical saplings, which developed normal wood tracheids with no S2L, is shown as a control.

Chapter 3

In situ detection of laccase activity and immunolocalization of a compression-wood-specific laccase (CoLac1) in differentiating xylem of _Chamaecyparis obtusa_

Abstract

The secondary cell wall of compression wood tracheids has a highly lignified region (S2L) in its outermost portion. To better understand the mechanism of S2L formation, I focused on the activity of laccase (a monolignol oxidase) and performed *in situ* studies of this enzyme in differentiating compression wood. Staining of differentiating compression wood demonstrated that laccase activity began in all cell wall layers before the onset of lignification. I detected no activity of peroxidase (another monolignol oxidase) in any cell wall layer. Thus, laccase likely plays the major role in monolignol oxidization during compression wood differentiation. Laccase activity was higher in the S2L region than in other secondary wall regions, suggesting that this enzyme was responsible for the high lignin concentration in this region of the cell wall. Immunolabeling demonstrated the expression of a compression-wood-specific laccase (CoLac1) immediately following the onset of secondary wall thickening; this enzyme was localized to the S2L region, whereas much less abundant in the S1 layer or inner S2 layer. Thus, the CoLac1 protein is most likely localized to the outer part of S2 and responsible for the high lignin concentration in the S2L region.

Introduction

Compression wood has anatomical and chemical characteristics that differ from those of normal wood (Wilson and Archer 1977, Timell 1986). These unique traits are believed to function in the generation of compressive growth stress (Yamamoto *et al.* 1991, Yamashita *et al*. 2007). Lignin content increases in compression wood cell walls; it is rich in *p*-hydroxyphenyl units and is especially abundant in the outer portion of the S2 layer (Timell 1986, Donaldson 2001). This highly lignified region is termed the “S2L” (Timell 1986), and its formation process has been a focus of interest because of the unique properties of compression wood (Fujita *et al.* 1978, Kim et al. 2010, Donaldson and Knox 2012). The lignin concentration in the S2L region is correlated positively with compressive growth stress (Okuyama *et al*. 1998). Therefore, elucidation of the mechanism by which the S2L forms will contribute to an improved understanding of compression growth stress generation.

Using molecular biological approaches, recent studies have shown that the proteins or RNAs of lignin synthesis genes are upregulated in differentiating compression wood (in comparison with differentiating normal wood) (Allona *et al*. 1998, Whetten *et al*. 2001, Koutaniemi *et al*. 2007, Yamashita *et al*. 2008, Yamashita *et al*. 2009, Villalobos *et al*. 2012). These modifications in gene expression are probably influential factors in S2L formation. I investigated the relationships between the transcript abundances of lignin synthesis genes (nine monolignol synthesis genes, two laccase genes, and one peroxidase gene) and S2L formation in *Chamaecyparis obtusa*. The Chapter 2 reported that the transcript abundance of a laccase gene (EC 1.10.3.2), which is involved in the oxidative polymerization of monolignol (Sterjiades *et al*. 1993, Ranocha *et al*. 1999, Berthet *et al*. 2011, Zhao *et al*. 2013, Barros *et al*. 2015), was correlated closely with S2L thickness, but this was not the case for other genes involved in monolignol synthesis. Moreover, this laccase gene (annotation *CoLac1*: accession number, AB762662) was highly expressed in differentiating compression wood, but not in differentiating normal wood (Chapter 2). This compression-wood-specific gene appeared to have crucial functions in the formation of specific compression wood features, such as the S2L. Thus, laccase may play a key role in S2L lignification.

McDougall (2000) compared the proteins extracted from differentiating compression wood with those from normal wood and found that one laccase protein was especially abundant in differentiating compression wood. However, the *in vitro* laccase activity of the extract did not differ between compression and normal woods, probably because the samples included all differentiating stages, thereby obscuring any difference. Consequently, an *in situ* analysis that discriminates among the stages of differentiation is required for the evaluation of laccase function during the differentiation of compression wood.

In our *in situ* study, I investigated laccase in the differentiating compression wood of *C. obtusa* saplings. I differentially stained laccase activity in the sections to localize the enzyme and its action. Plant peroxidase (EC 1.11.1.7) is also involved in the oxidative polymerization of lignin (Sterjiades *et al*. 1993, Fagerstedt *et al*. 2010, Shigeto *et al*. 2013, Barros *et al*. 2015). I therefore assessed the activities of peroxidase and laccase. I concurrently observed the lignin deposition process in differentiating xylem using ultraviolet microscopy (Fergus *et al*. 1969, Yoshida *et al*. 2002, Yoshinaga *et al*. 2012) and determined the relationship between laccase activity and the lignin deposition process. Finally, I observed the localization of compression-wood-specific laccase (CoLac1 protein) in differentiating compression wood using immunolabeling. Based on our findings,

I discuss the function of laccase in S2L formation, with a particular focus on the function of the CoLac1 protein.

Materials and methods

Plant material

Twelve *Chamaecyparis obtusa* saplings (each approximately 1.5 m tall) were used. Six of these were grown at an angle (*i.e.*, with non-vertical stems) for approximately two months (April–June), to generate compression wood. The other six saplings were grown vertically and formed normal wood.

Three of the six saplings with compression/normal wood were used for *in situ* studies; one sapling was used for each of three assays (peroxidase activity, the relationship between laccase activity and lignin deposition, and Colac1 localization). Selected pieces of stem that included differentiating compression wood were harvested from the saplings and cut with a razor blade into small square blocks measuring several millimeters on each side. These blocks were subjected to peroxidase-laccase activity staining, laccase activity staining, and immunolabeling, as described below.

The other three saplings with compression/normal wood were used for protein extraction. The stems of the saplings were cut into segments and the differentiating secondary xylem in the cut portions harvested using a chisel. Immediately after harvesting, the differentiating secondary xylem fragments were frozen in liquid nitrogen and stored at −80°C for protein extraction.

Detection of laccase and peroxidase activities in differentiating xylem

The blocks stained for laccase activity (shown in Figure 4) were prepared as follows: Blocks were treated with catalase in Tris-buffered saline (TBS; pH 7.6) for 30 min to remove H_2O_2 and prevent peroxidase activity. They were then immersed overnight in laccase activity staining buffer (0.5 mM 3,3'-diaminobenzidine-tetrahydrochloride [DAB], 100 μg/mL catalase in TBS) at 30°C.

The blocks stained for peroxidase-laccase activity (Figure 4) were treated with peroxidase-laccase activity staining buffer (0.5 mM DAB, 10 mM H_2O_2 in TBS) without catalase treatment. Pine laccases, expressed in differentiating normal wood, have maximal activity at pH 5.0 (Sato *et al.* 2006). TBS buffer (pH 7.6) is commonly used for horseradish peroxidase (HRP)

oxidization. A Tris buffer (pH 7.5) similar to TBS (pH 7.6) has been used to study the peroxidase involved in xylem lignification in *Populus alba* and *A. thaliana* (Shigeto *et al*. 2012, 2014). Therefore, TBS (pH 7.6) was used as the reaction buffer for laccase and peroxidase-laccase activity staining to avoid the optimum pH for laccase activity (pH 5.0), while promoting peroxidase activity. Some of the cut blocks were autoclaved to inactivate enzyme activity; these were used as negative controls. The blocks were immersed overnight in peroxidase-laccase activity staining buffer at 30°C. Each small block was cut transversely in half to obtain corresponding sections of differentiating xylem for paired analyses of laccase activity and ultraviolet microscopic observations (shown in Figure 5). The laccase activity staining image was obtained from one of the twin block portions by applying the same staining procedure used to generate the image in Figure 4, but I changed the pH of the reaction buffer by switching to a sodium acetate-acetic acid buffer (pH 5.0, at which pine laccases that express in secondary xylem have maximum activity levels; Sato *et al*. 2006).

After staining for enzyme activity, I fixed the blocks in 3% glutaraldehyde in phosphate buffer (pH 7.0) and embedded them in LR White resin. I cut 1-μm-thick sections from the top of the transverse plane of each block and examined each by light microscopy. I also observed the same section by polarizing microscopy to identify the cells that began secondary wall thickening.

Ultraviolet microscopy

The second member of each twin block pair was fixed with 3% glutaraldehyde in phosphate buffer (pH 7.0) and embedded in epoxy resin (Quetol-812; Nisshin EM, Japan). I cut a 1-μm-thick section from each block and examined it by ultraviolet microscopy. I obtained ultraviolet photomicrographs at a wavelength of 280 nm using ultraviolet microscopic spectrophotometers (MPM800; Carl Zeiss, Germany) equipped with ultraviolet-sensitive CCD cameras (CM-140 GE-UV; JAI, Denmark).

Protein extraction

I ground 5–10-g portions of differentiating xylem in liquid nitrogen to produce a powder. To obtain the soluble and ionically bound proteins, I extracted the differentiating xylem overnight in 50 mM sodium acetate-acetic acid buffer (pH 5.0) containing 1 M $CaCl_2$, 5% (w/v) polyvinylpyrrolidone, 0.5 mM phenylmethylsulfonyl fluoride, and 5 mM β-mercaptoethanol at 4℃. After extraction, the buffer was exchanged with 50 mM sodium acetate-acetic acid buffer (pH 5.0)

by dialysis, thereby removing the $CaCl_2$. The protein was concentrated using a Vivaspin 20 sample concentrator (GE Healthcare, USA). I determined protein concentrations by the Bradford procedure using bovine serum albumin (BSA) as the standard.

Native PAGE and in-gel laccase activity staining

The proteins extracted from differentiating xylem were separated using cathodic native PAGE (pH 4.4, β-alanine/acetate acid buffer, 8.0% acrylamide concentration). Following electrophoresis, the gel was immersed in sodium acetate-acetic acid buffer (pH 5.0) for 30 min, and then immersed overnight in laccase activity staining buffer (0.5 mM DAB and 100 μg/ml catalase in 50 mM sodium acetate-acetic acid buffer [pH 5.0]) at 35℃.

Western blotting

Anti-CoLac1 rabbit immunoglobulin G (IgG) antibody was designed for western blotting based on the amino acid sequence of the CoLac1 protein (RSQSLLPPPKDLPP); the peptide of this amino acid sequence was used as the antigen to raise the rabbit IgG antibody. The total amino acid sequence is available under accession number AB762662 (GenBank).

To combine the antibody and the peptide antigen, I mixed the anti-CoLac1 antibody and the antigen (peptide of RSQSLLPPPKDLPP), and incubated the mixture for 2 d. The proteins extracted from the differentiating xylem were separated by sodium dodecyl sulfate–PAGE (SDS-PAGE) (7.5%) and transferred to a polyvinylidine difluoride membrane (Immun-Blot PVDF membrane for protein blotting; BIO-RAD, USA). After washing the membrane in TBS containing 0.1% (v/v) Tween 20 (TBS-T), I immersed it in TBS-T containing 1% (w/v) BSA for 2 h at room temperature to block nonspecific antibody binding, and then washed it thrice for 15 min in TBS-T. The membrane was immersed overnight in anti-CoLac1 antibody or absorbed anti-CoLac1 antibody diluted 100-fold with TBS-T at 4℃, and then washed thrice for 15 min in TBS-T. Subsequently, I immersed the membrane for 90 min in anti-rabbit IgG, HRP-linked whole Ab goat (GE Healthcare) diluted 5000-fold with TBS-T at 35℃, and then washed it thrice for 15 min in TBS-T. ECL Prime (GE Healthcare) was used to generate chemiluminescence signals, which were detected with an LAS 3000 mini luminescent image analyzer (Fujifilm, Japan).

Immunolabeling

Square stem blocks, each several millimeters on a side, were frozen rapidly by immersion in liquid chlorodifluoromethane (HCFC-22) cooled with liquid nitrogen. The blocks were transferred into an acetone solution containing 0.7% glutaraldehyde cooled to –80℃, and then incubated for >2 d to obtain a frozen substitute. The blocks were incubated at –20℃ for 2 h, then at 4℃ overnight. After bringing the blocks back up to room temperature, I immediately washed them thrice for 10 min in acetone and then embedded them in LR White resin. I cut 1-μm-thick sections from the embedded blocks and immunolabeled them. Each section was first immersed in 50 mM glycin/phosphate-buffered saline (PBS) for 30 min, and then washed thrice for 15 min in PBS, followed by immersion in 0.8% (w/v) BSA/PBS for 1 h to block nonspecific binding. The sections were then washed thrice for 15 min in PBS. The anti-CoLac1 antibody used for western blotting was employed for immunolabeling. Each section was incubated in the anti-CoLac1 antibody diluted 10-fold in PBS for 3 d at 4℃, then washed thrice for 15 min in PBS, followed by incubation in secondary antibody (Alexa Fluor 647 goat anti-rabbit IgG [H+L] antibody; Life Technologies, USA) diluted 100-fold in PBS with 0.1% Tween 20 (PBS-T) for 1 h at 35℃. I shaded the sections from light during and after this treatment. The sections were washed thrice for 15 min in PBS-T, and mounted in Fluoromount/Plus medium (Diagnostic BioSystems, USA).

I detected Alexa 647 fluorescence in the sections by confocal laser scanning microscopy (FLUOVIEW FV10i; Olympus, Japan).

Results

Laccase and peroxidase activities in differentiating compression and normal woods

I observed laccase and peroxidase-laccase activities in differentiating secondary xylem by staining with DAB. In normal and compression wood sections, the differentiating tracheids were arrayed in a sequence of maturation from the cambium to mature tracheids (Figure 4A–F; left side is toward the bark, right side is toward the pith.). The cambium in compression wood sections developed many more differentiating tracheids than did that in normal wood sections; I distinguished differentiating tracheids by the presence of protoplasm (Figure 4A–F: dx). No *in situ* staining of peroxidase-laccase activity was visible in normal or compression wood samples that had been autoclaved (Figure 4A, D), but fresh samples were clearly stained (Figure 4B, C, E, F).

Laccase activity staining was visible in the phloem, differentiating xylem (Figure 4B, E). Staining was visible in the compound middle lamellae (CML) and secondary walls of the differentiating

xylem (Figure 4B, E).

The separation of peroxidase activity from laccase activity in our samples was difficult because I was unable to remove oxygen, which is an electron acceptor in the oxidization mechanisms catalyzed by laccase. Therefore, I compared sections stained for laccase and peroxidase activity (peroxidase-laccase activity staining) with sections stained only for laccase activity; this procedure allowed us to localize peroxidase activity. In differentiating compression and normal woods, protoplasm stained for peroxidase-laccase activity was more strongly pigmented than protoplasm stained for laccase activity alone, but this was not the case for the cell walls at any stage in the differentiation process (compare Figure 4C and Figure 4B [compression wood] with Figure 4F and Figure 4E [normal wood]).

The bordered pits in mature normal wood stained strongly for peroxidase-laccase activity (Figure 4G with Figure 4H), but those in differentiating and mature compression wood did not stain strongly for peroxidase-laccase activity. Cell wall laccase activity was higher in differentiating compression wood than in normal wood; this difference between the two types of wood was especially marked in the secondary walls (Figure 4B, E).

Relationship between laccase activity and lignin deposition in compression wood

The images in Figure 5A, and B demonstrate the relationship between laccase activity and lignin deposition in differentiating compression wood. The negative controls were autoclaved to inactivate laccase activity; no staining was observed in sections prepared in this manner (not shown). Laccase activity was always present in the CML and secondary wall prior to the onset of lignin deposition.

In cambium and expansion cells (cambium–0), laccase activity was observable in the CML (Figure 5A: cambium–0). No lignin deposition was detected in these cells (Figure 5B: cambium–0'). During S1 formation (cells 1–2), laccase activity was detected in the S1 layer; enzyme activity levels were high in the newly formed cell wall (Figure 5A: 1–2). Lignin deposition was first observed in the CML (Figure 5B: 1'–2'), where laccase activity had previously been detected prior to S1 thickening (Figure 5A: cambium–0).

Early in S2 formation (cells 3–4), laccase activity was detected in the S2 layer; higher activity was detected in the S2L region (Figure 5A: 3–4, arrow). Lignin was deposited in the S1 layer (Figure 5B: 3'–4'), where laccase activity had been detected during S1 formation (Figure 5A:

1–2). Laccase activity in the S1 layer diminished after lignification (Figure 5A: 3–4, arrowhead; Figure 5A, 1–2).

Late in S2 formation (cells 5–7), laccase activity was detected in the S2 layer; activity was highest in the outer portion of this layer (Figure 5A: 5–7). Laccase activity was also high near the innermost layer of S2 (Figure 5A: helical ribs). During thickening, the lignin content increased in the outer region of S2 (Figure 5B: 5'–7'), where laccase activity had been high during the early stages of S2 formation (Figure 5A: 3–4, arrow).

As cells lost their protoplasm, laccase activity in S2 fell below the level present in cells at earlier differentiation stages (Figure 5A: 8–10); lignin deposition in S2 fell sharply at the same time (Figure 5B: 8'–10').

Relationship between laccase activity and lignin deposition in normal wood

The timing of laccase activity relative to lignin deposition was similar in both normal and compression wood. Laccase activity was detected in the CML and secondary walls of normal wood before the onset of lignin deposition.

In cambium and expansion cells (cambium-0), laccase activity was observed in the CML of differentiating xylem (Figure 5C: cambium–0), but no lignin deposition was detected in these cells (Figure 5D: cambium–0').

During S1 formation (cell 1), laccase activity was detected in the CML and the S1 layer (Figure 5C: 1). Lignin deposition began in the CML (Figure 5D: 1'), where laccase activity had been detected prior to S1 thickening (Figure 5C: cambium–0).

Early in S2 formation (cell 2), laccase activity was detected in the S2 layer (Figure 5C: 2). Lignin was deposited in the lamella and the S1 layer (Figure 5D: 2'), where laccase activity had been detected during S1 formation (Figure 5C: 1).

Late in S2 formation (cell 3), laccase activity was low in the secondary wall, but often high in the innermost wall layers (Figure 5C: 3). Lignin deposition in the secondary walls began (Figure 5D: 3') where laccase activity had previously been detected during S2 formation (Figure 5C: 2). Laccase activity was reduced in the middle lamella, where lignin deposition was nearly complete (Figure 5C: 3; Figure 5D: 3').

Finally, laccase activity decreased in cells losing their protoplasm (Figure 5C: 4–6) as lignin was deposited in their secondary walls (Figure 5D: 4'–6').

Differences in laccase proteins between differentiating compression and normal woods

Proteins extracted from the two types of wood were separated by polyacrylamide gel electrophoresis (PAGE), and laccase activities in the gels were detected by staining (Figure 6). The electrophoretic mobilities of laccases in differentiating compression and normal woods differed. At least four laccases (bands a–d) were detected in differentiating compression and normal woods. Band c was detected in all compression wood samples, but in none of the normal wood samples. Band b was detected in all normal wood samples, but in none of the compression wood samples.

Western blot analysis using the anti-CoLac1 antibody

I performed an anti-body absorption test to determine whether the anti-CoLac1 antibody bound specifically to the CoLac1 protein (Figure 7A). Using a combination of the antibody and peptide antigen, I performed western blot analyses against proteins extracted from differentiating xylem and compared the results with those obtained with the anti-CoLac1 antibody. When I used the anti-CoLac1 antibody, I detected a single band in the size range of 100–130 kDa (Figure 7A: lanes labeled "anti-CoLac1 antibody"). However, I did not detect this band when the anti-CoLac1 antibody was absorbed into the peptide antigen (Figure 7A: lanes labeled "absorbed").

Proteins to which the anti-CoLac1 antibody had bound were detected among those extracted from differentiating compression wood, but not among those extracted from normal wood (Figure 7B: compare "compression wood" and "normal wood" lanes). I detected one obvious signal and one very weak signal in each of the compression wood samples (Figure 7B: "compression wood" lanes). I detected a single signal in the laccase purified from band c in Figure 6 (which was expressed in compression wood, but not in normal wood; Figure 7B: "L" lane). This protein was in the 100–130 kDa size range and clearly matched the protein in differentiating compression wood (Figure 7B: "compression wood" and "L" lanes).

Immunolocalization of CoLac1 protein in compression wood

When a compression wood section was treated with the anti-CoLac1 antibody, I observed a strong Alexa 647 signal in the differentiation xylem (Figure 8A). The co-occurrence of an Alexa 647 signal and lignin fluorescence in the same section indicated that (i) the Alexa 647 signal had started to appear immediately prior to lignification in the CML (Figure 8A, B) and (ii) the signal had

localized to the cell wall, and not the protoplasm (Figure 8A). I detected no Alexa 647 signal when the compression wood section was prepared without the anti-CoLac1 antibody (Figure 8C).

When the normal wood section was treated with the anti-CoLac1 antibody, I detected a scattered, weak Alexa 647 signal in the differentiating xylem (Figure 8E). No Alexa 647 signal was detected when the normal wood section was prepared without the anti-CoLac1 antibody (Figure 8G).

Discussion

In situ detection of laccase activities in differentiating normal and compression woods

When laccase and peroxidase were inactivated by autoclaving, I observed no staining (Figure 7A, D), but without this inactivation treatment, differentiating phloem and xylem were clearly stained (Figure 4B, C, E, F). Hence, the staining was indicative of laccase and peroxidase activities. Bao *et al*. (1993) used a similar method to investigate laccase activity in differentiating xylem sections of *Pinus taeda*. They immersed a 30-μm-thick section in diaminofluorene to stain the tissue, and found that differentiating xylem had higher laccase activity than mature xylem (*loc*. *cit*.). In the present study, I immersed a fresh xylem block in the DAB substrate prior to cutting 1-μm-thick sections. Our thin-sectioning procedure allowed us to observe the different stages of tracheid differentiation (Figure 4A–F) and to roughly separate the cell wall layers (Figure 5A, C).

Laccase activity staining of the sections produced pigmentation in the cell walls (Figure 4B, E), indicating that the enzymes were localized to the cell walls during cellular differentiation of tracheids. Cell wall laccases and peroxidases oxidize monolignols in the process of lignin deposition as cells differentiate (Donaldson 2001, Vanholme *et al*. 2010, Barros *et al*. 2015). Our staining localization of laccase activity was congruent with this concept.

Laccase activity was higher in the walls of compression wood cells than in the walls of normal wood cells (Figure 4B–E), suggesting that the lignin content in compression wood is higher than that in normal wood because of the difference in cell wall laccase activity between the two types of wood.

In situ detection of peroxidase activities in differentiating normal and compression woods

The intensity of peroxidase-laccase staining exceeded that of laccase staining in the protoplasms of normal and compression woods (cf. Figure 4C and Figure 4B [compression wood], and Figure 4F and Figure 4E [normal wood]). The intense protoplasmic staining may be attributed to

peroxidase activity. Thus, peroxidases were localized to the protoplasm of differentiating normal and compression woods. The laccases and peroxidases that are localized to cell walls oxidize monolignols during the process of lignin deposition (Donaldson 2001, Vanholme *et al*. 2010, Barros *et al*. 2015). Therefore, the peroxidases localized to the protoplasm (Figure 4) were not involved in lignin deposition. Plant peroxidase has a broad range of functions (Cosio and Dunand 2009), including the removal of hydrogen peroxide from the protoplasm. Our staining procedures indicated that peroxidase activity appeared weaker than laccase activity in the cell wall during lignification (cf. Figure 4C and Figure 4B [compression wood], and Figure 4F and Figure 4E [normal wood]), suggesting that peroxidase does less participate in monolignol oxidization in *C*. *obtusa*. Sterjiades *et al*. (1993) reported that oxidases other than peroxidase (e.g., laccase) may be involved in the early stages of lignification, and that peroxidase may be involved at a later stage. However, our staining procedures indicated that laccase was involved in the entire lignification process in *C*. *obtusa*. Previous studies using mutants of *Arabidopsis thaliana* indicated that laccase (Berthet *et al*. 2011, Zhao *et al*. 2013) and peroxidase (Shigeto *et al*. 2013, 2015) are involved in the lignification of the stem. Thus, angiosperms may have developed a lignification mechanism that functions via peroxidase oxidization.

Relationships between (i) laccase localization and changes in its activity and (ii) lignin deposition

In normal and compression woods, lignin was deposited in the cell corners and CML at the onset of secondary wall thickening (Figure 5B, D). Lignin was deposited in the unlignified secondary wall as it thickened, as shown in previous studies (Fujita *et al*. 1978, Takabe *et al*. 1981).

Laccase activity started before the onset of lignification in the CML and all cell wall layers of differentiating compression wood (Figure 5A, B), which would be predicted if laccase were responsible for the oxidation of monolignol during the process of lignin deposition. Furthermore, laccase activity was higher in the S2L region during and after the process of thickening (Figure 5A: cells 3–7). This localization of laccase activity to the secondary wall was related closely to lignin distribution. Thus, elevated laccase activity probably promotes the development of high lignin concentrations in the S2L region, resulting in S2L formation. Laccase activity was high in the proximity of the innermost layer of S2 (Figure 5A: cells 5–7). Compression wood tracheid forms helical ribs at the lumen of the cell wall (Wilson and Archer 1977, Timell 1986). Thus, the laccase

activity observed in the proximity of the innermost layer of S2 is probably located in the helical ribs. Function of the high laccase activity at the helical ribs is unclear, because lignin concentration in this part is not higher than in the other S2 regions (Figure 5B: cell 10).

Laccase activity began in the unlignified walls of newly formed differentiating compression wood cells (Figure 5A: cells 1–7), suggesting that laccase was accumulated concurrently with the formation of unlignified cell walls. Laccase activity in each of the wall regions weakened as lignin was deposited, and finally shut down (Figure 5A). Laccase activity may have been lost during monolignol oxidation. Alternatively, laccase activity staining may have weakened because lignin obstructed the passage of the substrate to the laccase located in the cell wall.

The initial recognition of laccase as a potential monolignol oxidase was based on biochemical evidence (Sterjiades *et al*. 1993). Biological evidence (based on studies of *A. thaliana* mutants) also indicates that laccase is involved in lignin deposition (Berthet *et al*. 2011, Zhao *et al*. 2013). Berthet *et al*. (2011) showed that AtLac4 and AtLac17 proteins are localized to the cell wall or CML, but there is a dearth of detailed information on the lignification process (e.g., expression timing during cell wall formation and differences in localization and activities among the cell wall layers). I showed that the relationship between laccase activity and lignin deposition provides crucial information on cell wall lignification, i.e., histochemical evidence for lignin deposition via laccase oxidization.

In normal and compression woods, laccase activity was related closely to the timing of lignin deposition. However, the in-gel analysis of laccase activity detected different laccase proteins between differentiating compression and normal woods (Figure 6), indicating that *C. obtusa* modifies laccase expression during the differentiation process in compression wood, which may account in part for the differences in lignin content and distribution between compression and normal woods.

Assessment of anti-CoLac1 antibody specificity

I performed western blotting to assess the specificity of the anti-CoLac1 antibody. When the anti-CoLac1 antibody was used, I detected a single band in each compression wood sample (Figure 7A: “anti-CoLac1 antibody” lanes), but no band was detected when the anti-CoLac1 antibody was absorbed into the peptide antigen (Figure 7A). Thus, the anti-CoLac1 antibody recognized the peptide sequence of CoLac1 (RSQSLLPPPKDLPP) and bound to a protein that

included this peptide sequence. The same band was detected in compression wood (with no obvious extra band; Figure 7B: "compression wood" lanes). Therefore, the anti-CoLac1 antibody bound to a single protein among the soluble and ionically bound proteins I extracted from differentiating compression wood. The protein with laccase activity that we extracted from differentiating compression wood (Figure 6: band c) and purified from the gel used in the native PAGE procedure was detected in the same band (Figure 7B: "L" lane). Thus, the protein in the band had laccase activity and was specific to differentiating compression wood. It was not found in normal wood. The following conclusions may be drawn. The single protein to which the anti-CoLac1 antibody bound included the peptide sequence of CoLac1 (RSQSLLPPPKDLPP); it was expressed in differentiating compression wood, but not in differentiating normal wood, and it had laccase activity. Thus, our western blotting demonstrated that the anti-CoLac1 antibody bound specifically to CoLac1 protein.
The protein was in the 100–130 kDa size range. Our findings were congruent with those of a SDS-PAGE study, which detected a 120 kDa protein specific to the differentiating compression wood of Sitka spruce (McDougall 2000). However, the putative protein size of CoLac1, which comprises 580 amino acids, is about 60 kDa (excluding a putative signal peptide). Most laccases in *A. thaliana* have high isoelectric points (McCaig *et al*. 2005). The ExPASy - Compute pI/Mw tool (http://web.expasy.org/compute_pi/) predicted a high isoelectric point (9.2) for the CoLac1 protein, and the NetNGlyc (http://www.cbs.dtu.dk/services/NetNGlyc/) service predicted 22 N-glycosylation sites (Asn-Xaa-Ser/Thr sequons). Therefore, the inconsistency in protein size estimates (100–130 kDa *vs*. 60 kDa) may have arisen from a reduction in electrophoretic migration caused by the protein's high isoelectric point and glycosylation pattern.

Localization and function of CoLac1 protein in differentiating compression wood

I used immunolabeling with the anti-CoLac1 antibody to investigate localization of the CoLac1 protein (Figure 8). I observed an Alexa 647 signal when a section was treated with the anti-CoLac1 antibody (Figure 8A), but no signal appeared in the absence of the antibody (Figure 8C). Therefore, the Alexa 647 signal was indicative of CoLac1 protein localization.

In the compression wood section, the Alexa 647 (CoLac1) signal started to appear immediately prior to lignification in the CML (Figure 8A, B), concurrent with the onset of thickening in the S1 layer (Figure 5A, B). Therefore, the CoLac1 protein was expressed when S1 thickening began, but laccase activity was observable even earlier (Figure 5A: cambium–0). Thus,

laccases other than the CoLac1 protein were expressed and localized in the CML. The CoLac1 protein was active in the secondary wall, but not in other cell wall layers.

The localization of the CoLac1 signal differed between normal wood and compression wood sections. When a normal wood section was treated with the anti-CoLac1 antibody, a very weak, scattered CoLac1 signal appeared with no particular localization (Figure 8E); when the antibody was excluded from the treatment, no CoLac1 signal was observed (Figure 8G). Thus, the CoLac1 protein was not localized to any particular region in differentiating normal wood. The very weak CoLac1 signal in normal wood may have resulted from the nonspecific binding of the anti-CoLac1 antibody. Earlier work demonstrated laccase expression in differentiating compression wood, but not in differentiating normal wood (McDougall2000, Chaapter 2). Our immunolabeling procedure also indicated that the CoLac1 protein was expressed in differentiating compression wood and not in differentiating normal wood.

The CoLac1 signal first appeared in the innermost region of the thickening secondary wall of compression wood (Figure 8I: cell 1), and appeared subsequently in the thickened S2 layer(Figure 8I: cell 4), suggesting that the CoLac1 protein was introduced into the compression wood cell wall during secondary thickening and became localized in the secondary wall thereafter. The CoLac1 signal appeared in a ring formation in the secondary walls of mature compression wood (Figure 8K); this ring formation coincided with the distribution of a highly lignified region (S2L; Figure 8K, L; arrows). Thus, the CoLac1 protein was eventually localized to the S2L region, suggesting that the high lignin concentration in this region results from monolignol oxidization by this protein. The CoLac1 signal was scattered in the inner layer of S2 (Figure 8K). The CoLac1 protein was also localized to this region, but was much less abundant there than in the S2L region.

The CoLac1 protein was involved in S2L formation, as described above. The functional mechanism of S2L formation may be complex. Hemicellulose distribution differs between the cell walls of compression and normal woods (Donaldson and Knox 2012); galactan is distributed in the S2L region (Altaner *et al*. 2010, Kim *et al*. 2010, Donaldson and Knox 2012). Hemicellulose likely provides appropriate conditions for lignin deposition (Terashima *et al*. 1989, 1993). Therefore, modifications of the hemicellulose types and their distributions may play a role in S2L formation.

S2L formation is probably important in the generation of compressive growth stress, and the CoLac1 protein may generate this form of stress independently. The stress generation mechanism has been explained by the “lignin swelling hypothesis” proposed by Boyd (1972). According to this

theory, a combination of high lignin content and a steep microfibril angle in the S2 layercauses axial compressive growth stress. The S2L region appears to be particularly important in this context, as its lignin concentration is correlated positively with compressive growth stress (Okuyama *et al*. 1998). If a compression-wood-specific laccase (CoLac1) knockdown mutant were to be produced, I predict that it would form compression wood with a low lignin content and low levels of lignification in the S2L region. Further studies in this direction will contribute crucial information on the biomechanics of ideal shape formation in trees.

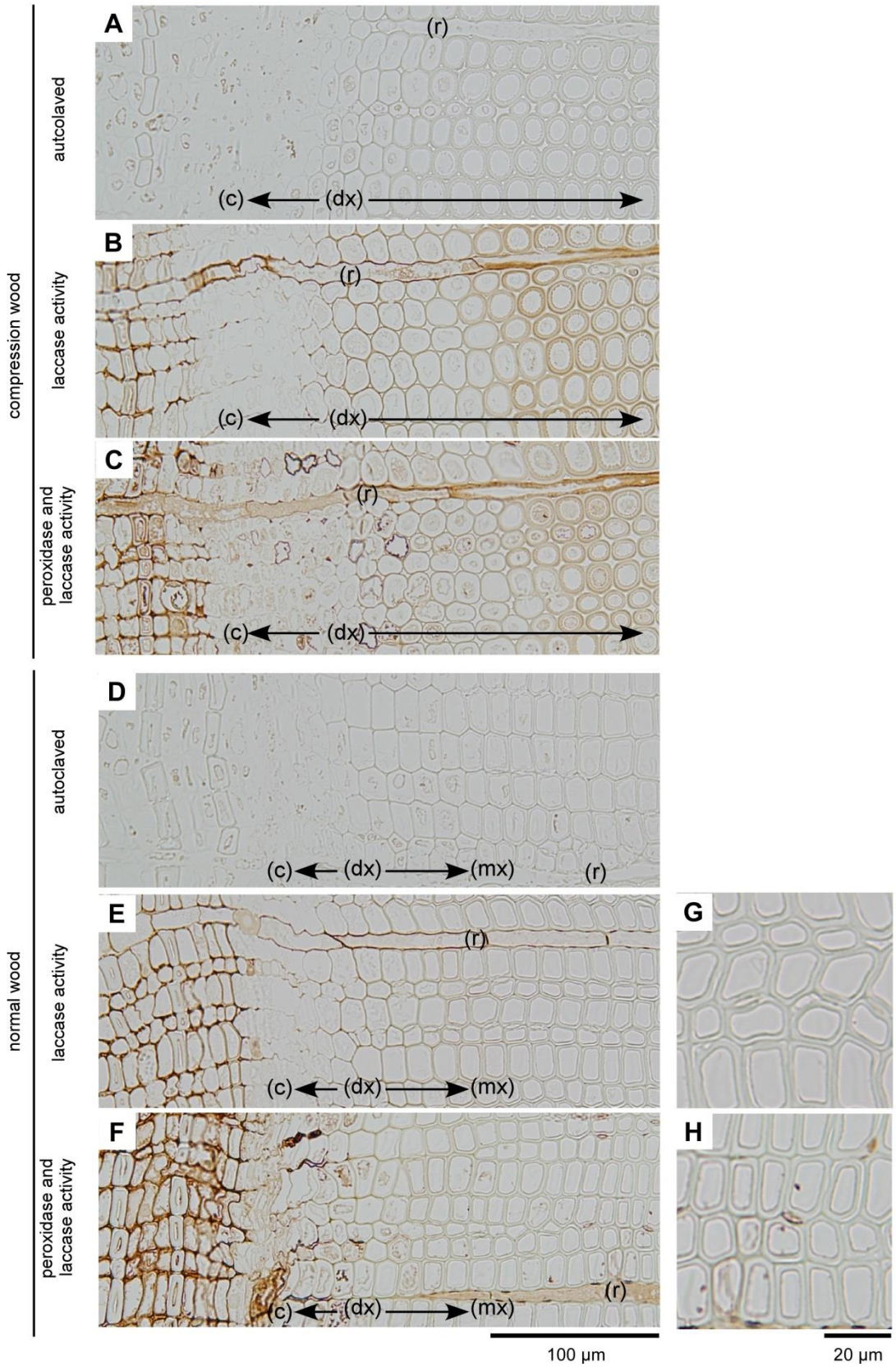

Figure 4. Laccase and peroxidase activities detected *in situ* in differentiating xylem. A)

Compression wood section autoclaved and stained for peroxidase-laccase activity. B) Compression wood section stained for laccase activity. C) Compression wood section stained for peroxidase-laccase activity. D) Normal wood section autoclaved and stained for peroxidase-laccase activity. E) Normal wood section stained for laccase activity. F) Normal wood section stained for peroxidase-laccase activity. G) Enlargement of the area around the bordered pit in E. H) Enlargement of the area around the bordered pit in F. c, cambium; dx, differentiating xylem; mx, mature xylem; r, ray parenchyma.

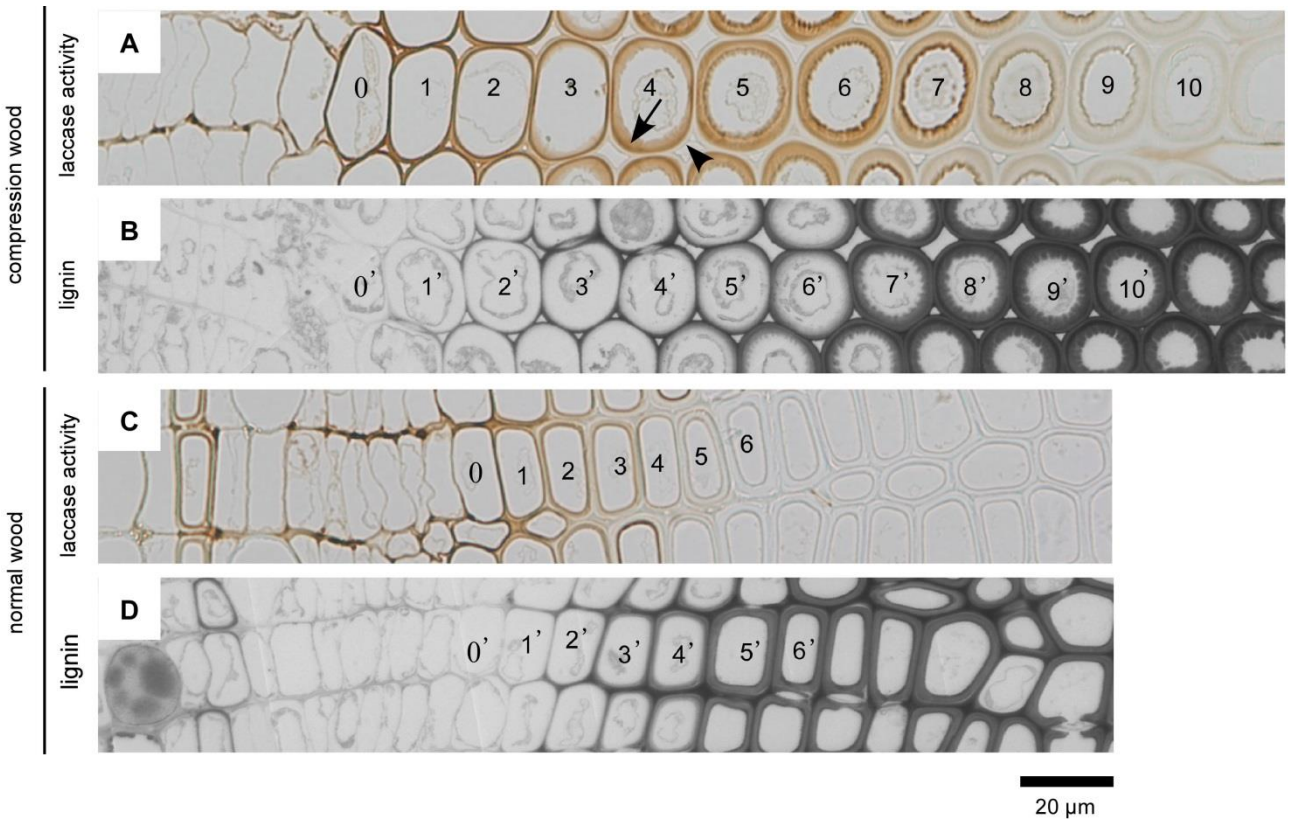

Figure 5. Relationship between laccase activity and lignin deposition. A) Compression wood section stained for laccase activity. B) Ultraviolet microscopic image of a compression wood section. C) Normal wood section stained for laccase activity. D) Ultraviolet microscopic image of a normal wood section. In each image, the secondary walls of cells labeled "1, 1'" are at the earliest stage of thickening (confirmed by polarizing microscopy; Fujita *et al*. 1978, Takabe *et al*. 1981). Cells in A – D are labeled "0–10, 0'–10'" in order of maturation, using those labeled "1, 1'" as a standard. In A, B: "cambium-0, cambium-0'", expansion cells comprising a primary cell wall and middle lamella; "1–2, 1'–2'", S1 formation; "3–4, 3'–4'", early S2 formation; "5–7, 5'–7'", late S2 formation (helical ribs); "8–10, 8' –10'", disappearing protoplasm (mature stage). In C, D: "cambium-0, cambium-0'",

expansion cells comprising a primary cell wall and middle lamella; "1, 1'", S1 formation; "2, 2'", early S2 formation; "3, 3'", late S2 formation; "4–6, 4'–6'", disappearing protoplasm (mature stage). Arrows and arrowheads indicate outer regions of S2 and S1 layers, respectively.

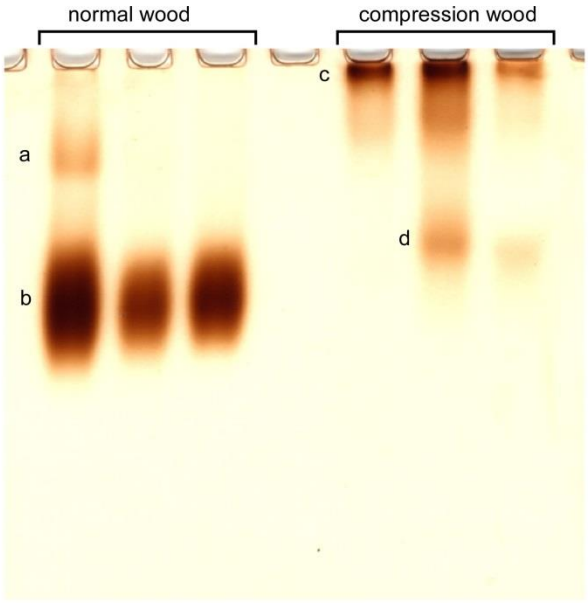

Figure 6. Differences in laccases extracted from differentiating xylem between compression and normal woods. Native polyacrylamide gel electrophoresis and in-gel laccase activity staining were used to visualize differences in enzyme characteristics between wood types. Bands a-d indicate different proteins. Band c was detected in all compression wood samples, but in none of the normal wood samples. Band b was detected in all normal wood samples, but in none of the compression wood samples.

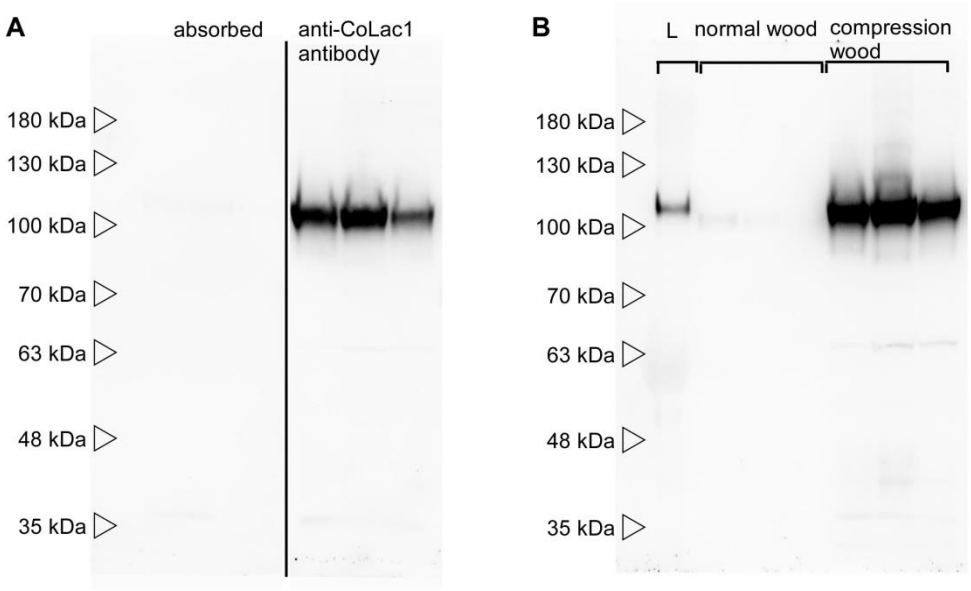

Figure 7. Western blotting to assess antibody specificity. A) Antibody absorption of the anti-CoLac1 antibody. No signal was detected to the left side of the membrane (absorbed). A single signal was detected in each lane to the right side of the membrane (anti-CoLac1 antibody). B) Detection of proteins sensitive to the anti-CoLac1 antibody among compression wood proteins, normal wood proteins, and compression wood-specific laccase protein (band c protein in Figure 6; labeled "L" on the membrane).

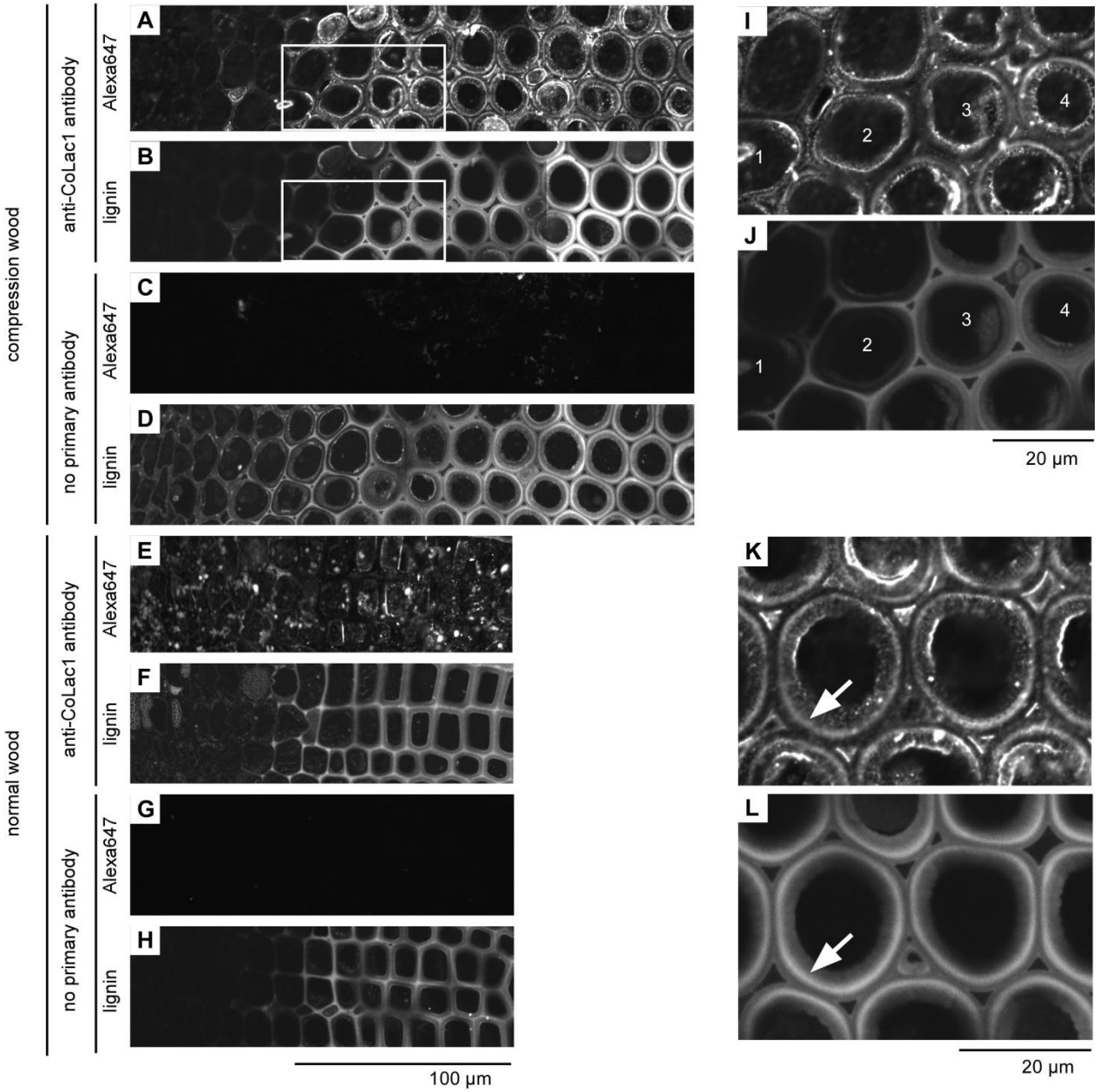

Figure 8. Immunolocalization of CoLac1 protein in differentiating compression wood. A) Alexa 647 fluorescence in a compression wood section treated with anti-CoLac1 antibody. B) Lignin intrinsic fluorescence in the section shown in A. C) Alexa 647 fluorescence in a compression wood section treated without the anti-CoLac1 antibody. D) Lignin intrinsic fluorescence in the section shown in C. E) Alexa 647 fluorescence in a normal wood section treated with anti-CoLac1 antibody. F) Lignin intrinsic fluorescence in the section shown in E. G) Alexa 647 fluorescence in a normal wood section treated without anti-CoLac1 antibody. H) Lignin intrinsic fluorescence in the section shown in G. I) and J) Enlargements of thickened secondary walls in the cell images shown in A and B, respectively.

The cells are ordered in the sequence of maturation (1–4). K) Alexa 647 fluorescence in mature compression wood shown in A. L) Lignin intrinsic fluorescence in the section shown in K. Arrows indicate highly lignified regions in the S2 layer in L.

Chapter 4

Common mechanism of lignification of compression wood in conifers and *Buxus*

Abstract

Woody plants develop a specialized secondary xylem known as reaction wood to enable formation of an ideal shape. Reaction wood in coniferous species is known as compression wood, and that of woody angiosperms as tension wood. However, the genus *Buxus*, which is classified as an angiosperm, forms compression-wood-like reaction wood. I investigated the mechanism of lignification in coniferous compression wood and *Buxus* reaction wood. [i] Several lignin synthesis genes were upregulated in differentiating reaction wood of *Buxus microphylla*; [ii] *B. microphylla* possesses a specific laccase gene that is expressed specifically in differentiating reaction wood (*BmLac4*); [iii] laccase activity localization was closely related to lignification of reaction wood, and laccase activity was high in the secondary wall middle layer; [iv] in reaction wood cell walls, galactan was present in the outer portion of the secondary wall middle layer, and the level of xylan was reduced. These findings suggest that lignification in *B. microphylla* reaction wood is identical to that of coniferous compression wood. These may represent general mechanisms of increasing lignin content in various reaction woods.

Introduction

In this Chapter, we focused on reaction wood of the genus *Buxus*. *Buxus* species are classified as angiosperms. Woody angiosperms generally develop reaction wood known as tension wood on the upper side of inclined stems and branches; tension wood is characterized by the presence of G fibers, which develop a cellulose-rich cell wall layer (the G layer) with a very small microfibril angle. However, *Buxus* species form no tension wood, and instead develop compression-wood-like reaction wood on the lower side of inclined stems and branches (Onaka 1949), which generates compressive growth stress (Bailleres et al. 1949). *Buxus* reaction wood is similar in chemical and anatomical features to compression wood (Onaka 1949, Bailleres et al. 1949); it shows eccentric growth on the lower side of inclined stems and branches; the xylem is darker brown than normal wood; the wood fiber and vessels in the transverse plane are circular; and the wood fiber has a large microfibril angle in the secondary wall, and an increased lignin content in the cell wall. Interestingly, the cell wall develops a highly lignified region in the outer portion of the secondary wall middle layer

(S2) (Yoshizawa et al. 1993), which is a remarkable characteristic of coniferous compression wood and known as S2L.

I investigated whether the lignification mechanism of *Buxus* reaction wood is identical to that of compression wood by assessing the lignification process in both *Buxus* reaction wood and coniferous compression wood. Molecular biological approaches have been used in previous studies to assess the mechanism of formation of compression wood (Allona et al. 1998 Whetten et al. 2001, Koutaniemi et al. 1998, Yamashita et al. 2008, Yamashita et al. 2009, Villalobos et al. 2012). The Chapter 2 and 3 reported that [i] expression of a laccase (CoLac1) in *Chamaecyparis obtusa* (a coniferous species) is very low in differentiating normal wood but very high in differentiating compression wood; [ii] laccase activity is higher in the S2L region than in other parts of the S2 layer; [iii] *Colac1* is expressed at the onset of secondary wall thickening and is localized to the S2L region. Based on these results, we concluded that a specific laccase (*CoLac1*) is localized in the S2L region, which results in a high lignin concentration in the S2L region in *C. obtusa*. Other previous studies suggested that the difference in hemicellulose type and distribution in compression wood might be involved in lignification (Donaldson and Knox 2012, Kim et al. 2010). Supposing the lignification mechanism of *Buxus* reaction wood to be identical to that of compression wood, this would be difficult to explain by the theory of convergent evolution. In this case, *Buxus* reaction wood also cannot be explained by this theory. In addition, our study provides fundamental information regarding compression wood formation and compressive growth stress generation, because the common mechanisms might be important for generating compressive growth stress.

In this study, I assessed the commonality of lignification by determining whether *Buxus* (*Buxus microphylla* var. japonica) possesses a specific laccase gene that is expressed specifically in differentiating reaction wood; whether *in situ* laccase activity in differentiating reaction wood is higher than that in normal wood, and if it is higher in the S2L region than the other S2 regions; and whether the distribution of hemicellulose (which is related to the lignin distribution) in the reaction wood cell wall is altered.

Materials and methods

Plant material

For cloning of genes involved in lignin synthesis, I used *Buxus microphylla* var. japonica grown at Nagoya University (~1.85 m tall). In mid-June, after bark had been removed from a branch,

differentiating xylem, which is a darker brown, was harvested from the lower side of the branch using a chisel, and was used as the reaction wood sample. Differentiating xylem was harvested from the upper side of the branch, and was used as the normal wood sample. In the same way, differentiating reaction and normal woods were harvested from four other branches for quantitative reverse transcript polymerase chain reaction (qRT-PCR) analysis.

For evaluation of laccase activity and ultraviolet microscopy, I harvested xylem blocks including differentiating reaction wood from the lower side of branches. Xylem blocks including differentiating normal wood were harvested from the upper side of these branches. The blocks were divided into small blocks of several millimeters square using a razor blade. To analyze similar sections of differentiating xylem for evaluation of laccase activity and for ultra violet microscopy, the small blocks were divided into two pieces in the transverse plane.

Buxus microphylla (~120-cm height, 5-cm base diameter) grown with the stem tilted at ~30° to induce formation of reaction wood was used for immunolabeling. Another plant was grown with the stem vertical to induce formation of normal wood. Xylem blocks including mature reaction wood were harvested from the lower side of the stem. Xylem blocks including mature normal wood were harvested from the vertical stems. Blocks were divided into small blocks of several millimeters square using a razor blade.

Gene cloning

Total RNA was purified from the differentiating xylem, and cDNA was synthesized using Primescript (TaKaRa, Japan). The target gene was amplified using degenerate primers (Chapter 2). The *B. microphylla* translation initiation factor (*BmTIF*, AB762681) gene was also amplified as a reference gene. The amplification product was inserted into a plasmid for DNA sequencing. The similarity of the sequence compared to that of *Arabidopsis thaliana* was investigated using The Arabidopsis Information Resource (TAIR) BlastX program. New sequences were submitted to the DNA Data Bank of Japan.

qRT-PCR

To investigate transcript abundance in differentiating normal wood and reaction wood, we performed qRT-PCR analysis. I harvested four branches from a *B. microphylla* tree, and shaved off the differentiating xylem from both the lower and upper side of the stem using a chisel. The samples were

immediately snap-frozen in liquid nitrogen, and the frozen differentiating xylem was stored at –80°C until RNA extraction. Total RNA was extracted from 50 mg of differentiating xylem using the RNeasy Plant Mini Kit (QIAGEN, Germany) according to the manufacturer's protocols, and treated with DNase I (TaKaRa, Japan) to remove contaminating genomic DNA. Absence of contaminating genomic DNA was confirmed by the failure of PCR amplification of the cyclophilin housekeeping gene (accession number, AB762680). The RNA concentration was estimated spectrophotometrically using Gene Quant (Amersham, Germany). cDNAs were synthesized at 37°C for 30 min with 500 ng of total RNA in a volume of 15 μL using PrimeScript RT Master Mix (Perfect Real Time; TaKaRa, Japan); the cDNAs were then diluted 3:10 with water.

Gene-specific primers were designed using the Primer 3 Plus program (http://www.bioinformatics.nl/cgi-bin/primer3plus/primer3plus.cgi); the sequences are shown in Table 4. Amplification was performed in triplicate using the StepOnePlus Real Time PCR System (Applied Biosystems, USA). The baseline and threshold cycles were determined automatically using the StepOne software ver. 2.1 (Applied Biosystems, USA). The 20-μL reaction mixture consisted of 0.5 μL cDNA, 200 nM sense and antisense primers, and 10 μL POWER SYBR Green PCR Master Mix (Applied Biosystems, USA). The reaction conditions were as follows: 95°C for 10 min (95°C for 15 s, 58°C for 60 s) × 40. To detect any additional products, after the melting curve was analyzed, I performed agarose gel electrophoresis and confirmed the absence of additional bands. The *BmTIF* gene was used as a reference gene; transcript abundance is expressed as the ratio of the target gene transcript to that of *BmTIF*.

Laccase activity staining

To analyze *in situ* laccase activity in differentiating xylem, I performed laccase activity staining using 3,3'-diaminobenzidine tetrahydrochloride (DAB) (Chapter 3). One of the twin blocks (see plant materials) was treated with catalase in sodium acetate-acetic acid buffer (pH 5.0) for 30 min to remove H_2O_2, preventing peroxidase activity. The blocks were immersed overnight in laccase activity staining buffer (0.5 mM DAB, 100 μg/mL catalase, in sodium acetate-acetic acid buffer [pH 5.0]) at 30°C. After activity staining, the blocks were fixed with 3% glutaraldehyde in phosphate buffer (pH 7.0), and embedded in LR White resin. Two-micrometer-thick sections were cut from the top of the transverse plane of the blocks, and observed under a light microscope. In addition, the same section was observed under a polarizing microscope to visualize cells that showed secondary wall

thickening (Fujita et al. 1978, Takabe et al. 1981).

Ultraviolet microscopic analysis

The other of the twin blocks (see plant materials) was fixed with 3% glutaraldehyde in phosphate buffer (pH 7.0), and embedded in epoxy resin. One-micrometer-thick sections were cut from the block and subjected to ultraviolet microscopy. Ultraviolet photomicrographs were taken at a wavelength of 280 nm using an ultraviolet microscopic spectrophotometer (MPM800, Carl Zeiss, Germany) equipped with an ultraviolet-sensitive CCD camera (CM-140 GE-UV, JAI, Denmark).

In addition, the same section was observed under a polarizing microscope to visualize cells that showed secondary wall thickening (Fujita et al. 1978, Takabe et al. 1981).

Immunolabeling

Stem blocks of several millimeters square were frozen rapidly by immersion in liquid chlorofluorocarbon cooled with liquid nitrogen. The blocks were transferred into acetone containing 0.7% glutaraldehyde cooled to –80°C, and incubated for at least 2 d for freeze substitution. The blocks were incubated at –20°C for 2 h and then at 4°C overnight. After the blocks had been warmed to room temperature, they were immediately washed in acetone three times for 10 min each, and then embedded in LR White resin.

One-micrometer-thick sections were cut from the embedded blocks, and used for immunolabeling. The sections were first immersed in 50 mM glycine/phosphate-buffered saline (PBS) for 15 min, and then washed three times for 5 min each in PBS. Sections were then immersed in 0.8% (w/v) bovine serum albumin/PBS for 1 h at room temperature to block nonspecific binding, and washed three times for 5 min each in PBS. Sections were incubated for 2 days at 4°C with LM5, LM10, or LM22 primary antibody (PlantProbes) diluted 50-fold in PBS, and washed three times for 10 min each in PBS, followed by incubation for 1 h at 35°C with the secondary antibody (Alexa Fluor 647 Goat Anti-Rat IgG (H+L) Antibody, Life Technologies) diluted 100-fold in PBS containing 0.1% Tween 20 (PBS-T). During and after this treatment, the sections were protected from light. The sections were washed three times for 10 min each in PBS-T, and developed with Fluoromount/Plus (Diagnostic BioSystems). Alexa647 fluorescence was visualized by confocal laser microscopy (FLUOVIEW FV10i, Olympus).

Results

Similarity of cloned *B. microphylla* genes to genes in the *Arabidopsis thaliana* genome

To estimate the functions of cloned *B. microphylla* genes, I investigated their sequence similarity to genes in the *A. thaliana* genome (Table 5). The cDNA sequences demonstrated similarity to genes encoding enzymes involved in lignin precursor (monolignol) synthesis, laccase, and TIF SUI1 family protein (63–93% identities; E-value, <E–5). The cloned sequences are available under the following accession numbers: *BmLac1* (AB762671), *BmLac2* (AB762672), *BmLac3* (AB762673), *BmLac4* (AB762674), *BmLac5* (AB762675), *BmPAL1* (AB762676), *BmCAD1* (AB762677), and *BmTIF* (AB762681).

Comparison of transcript abundance between differentiating reaction and normal woods

To compare the gene expression levels in differentiating reaction wood with those in differentiating normal wood, I performed qRT-PCT. Among laccase genes (*BmLac1–5*), *BmLac2* and *BmLac4* were expressed mainly in differentiating normal and reaction woods (Figure 9). Further analysis, which was more precise due to the use of four biological replicates, demonstrated a difference in transcript abundance between differentiating normal and reaction woods (Figure 10). The transcript abundance of *BmPAL* and *BmCAD* was higher in differentiating reaction wood (Figure 10). In contrast, the transcript abundance of *BmLac2* was not different between the two types of wood. The transcript abundance of *BmLac4* was very low in differentiating normal wood, but very high in differentiating reaction wood.

Laccase activity staining and lignin deposition in differentiating reaction wood

To investigate lignin deposition in differentiating reaction wood, I performed ultraviolet microscopy. In the micrographs, lignin appears dark; thus darker regions indicate higher lignin concentrations (Fergus et al. 1969, Yoshida et al 2002, Yoshinaga et al. 2012). Asterisks indicate cells that have begun secondary wall thickening (confirmed by polarizing microscopy (Fujita et al. 1978, Takabe et al. 1981)). In addition, to investigate *in situ* laccase activity in differentiating reaction wood, I performed laccase activity staining (Figure 11 A, B, D, F), in which a brown color shows laccase activity (Chapter 3). The negative control was autoclaved to inactivate laccase activity; no staining was observed in sections prepared in this manner (Figure 11 A, D).

Laccase activity was initiated in the compound middle lamella and cell wall layers of

secondary walls in all regions prior to the onset of lignin deposition, as described below. In differentiating reaction wood, staining was observed in the compound middle lamella before the onset of secondary wall thickening (Figure 11 B: c, e), while lignin deposition was not observed (Figure 11 C: c, e). Staining was observed in the secondary wall outer layer (S1) immediately after the onset of the secondary wall thickening (Figure 11 B, asterisk), when lignin was deposited in the compound middle lamella (Figure 11 B: asterisk). Staining appeared in the secondary wall middle layer (S2) during secondary wall thickening (Figure 11 B, s), when lignin was being deposited in the secondary wall (Figure 11 C: s). The staining in the cell wall was reduced with maturation after disappearance of protoplasm (Figure 11 B: mx), when lignin deposition was completed (Figure 11 C: mx). In mature cells, the outer region of S2 showed a higher lignin concentration than the inner region in mature cells (Figure 11 C: mx).

In differentiating normal wood, staining was observed in the compound middle lamella before the onset of secondary wall thickening (Figure 11 E: c, e), when lignin deposition was not observed (Figure 11 F: c, e). Staining was observed in the secondary wall immediately after the onset of secondary wall thickening (Figure 11 E: asterisk), when lignin was being deposited in the secondary wall (Figure 11 F: asterisk). Staining was evident in the secondary wall middle layer (S2) during secondary wall thickening (Figure 11 B, s), when lignin was being deposited in newly formed cell walls (Figure 11 C: s). The staining in the cell wall was reduced with maturation after disappearance of protoplasm (Figure 11 E: mx), when lignin deposition was completed (Figure 11 F: mx). During secondary wall thickening of reaction wood, the cell wall showed higher laccase activity in the secondary wall than that of normal wood (Figure 11 B, E: s). During secondary wall thickening of normal wood, the cell wall showed higher laccase activity in the innermost portion of the cell wall compared to other parts of the cell wall (Figure 11 B, E: s).

Distribution of hemicellulose in reaction wood

To investigate hemicellulose distribution in the cell wall, I performed immunolabeling using LM5, LM10, and LM21 antibodies, which are specific for galactan, xylan, and mannan, respectively. In mature reaction wood, LM5 labeling was observed not in S1, but in the outer part of S2 (Figure 12 A, C). In mature normal wood, little LM5 label was observed around the primary wall (Figure 12 B, D).

In mature reaction wood, LM10 was observed in S1 and S2, but the labeling density was low in the

outer part of S2 (Figure 12 E, G). In mature normal wood, LM10 labeling was observed in S1 and S2, and the labeling density in S1 was high (Figure 12 F, H).

In both mature normal and reaction wood, LM21 was observed in S2 (Figure 12 I, K, J, L); however, the labeling density was low in the central part of S2 in mature reaction wood (Figure 12 J, L).

Discussion

Differential expression of lignin synthesis genes between reaction and normal wood

Among the laccases of *B. microphylla* (*BmLac1–5*), *BmLac2* and *BmLac4* were expressed mainly in differentiating normal and reaction wood (Figure 9). This result suggested that laccases encoded by *BmLac2* and *BmLac4* function in differentiation into normal and reaction woods. A more-detailed analysis demonstrated that *BmLac2* expression is similar between normal and compression woods, but *BmLac4* expression is considerably higher in differentiating reaction wood than in differentiating normal wood (Figure 10). This result demonstrated that *B. microphylla* possesses a reaction-wood-specific laccase gene that is expressed during differentiation. In several coniferous species, laccase RNAs or proteins are upregulated in differentiating compression wood (Koutaniemi et al. 1998, Yamashita et al. 2008, Yamashita et al. 2009, Villalobos et al. 2012). Moreover, a compression-wood-specific laccase was found in *C. obtusa* (Chapter 2) and *Pinus radiata* (McDougall 2000). Thus, development of a specific laccase is common to *B. microphylla* and coniferous species.

Expression of *BmPAL* and *BmCAD* was higher in differentiating reaction wood than in differentiating normal wood (Figure 10). This suggests that differentiating reaction wood supplies a greater quantity of monolignol to increase lignin content. In coniferous species, the expression of genes involved in monolignol synthesis is upregulated in differentiating compression wood compared to that in normal wood (Allona et al. 1998, Whetten et al. 2001, Chapter 2). Thus, upregulation of monolignol synthesis genes is common to *B. microphylla* and coniferous species.

Relationship of laccase activity to lignin deposition and lignin distribution in the cell wall in reaction wood

In differentiating reaction wood, lignin deposition was not observed in any region before secondary wall thickening (Figure 11 C: c, e). At the onset of secondary wall thickening, lignin began

to be deposited in compound middle lamella (Figure 11 C: asterisk). During secondary wall thickening, lignin was being deposited to form the secondary wall (Figure 11 C: s). This lignin deposition process seems identical to that of compression wood of *Cryptomeria japonica* (Fujita et al. 1978). However, lignification in compound middle lamella is the exception; lignin is not deposited in the cell corner (intercellular space) in coniferous compression wood (Timell 1986), while lignin was deposited in this region in *Buxus* reaction wood (Figure 11 C: mx)

Lignin deposition was initiated after laccase activity appeared in the compound middle lamella, S1, and S2 in differentiating reaction wood (Figure 11 B, C), suggesting that laccase functions in lignification during differentiation into reaction wood in *B. microphylla*. I found that, in *C. obtusa*, laccase activity appeared prior to lignification in all cell wall layers in differentiating normal and compression wood (Chapter 3). This previous report coincides with the case of *B. microphylla*. Thus, participation of laccase oxidization in reaction wood lignification is a common feature of *Buxus* and coniferous species.

In differentiating reaction wood, laccase activity during lignification in the secondary wall was higher compared to that in normal wood (Figure 11 B, F: s). Our qRT-PCR analysis of a laccase gene (Figure 10: *BmLac4*) indicated that laccase activity in the reaction wood cell wall was higher than that in normal wood due to *BmLac4* expression, as demonstrated by laccase activity staining (Figure 11 B, E: s). The activity staining suggested that the higher laccase activity in the S2 layer is involved in the increase in lignin content in this region of reaction wood. In differentiating compression wood in *C. obtusa*, laccase activity is higher in the outer region of the S2 layer within the secondary wall, which results in a high lignin concentration in the S2L region (Chapter 3). Thus, the relationship between laccase activity intensity and lignin deposition in the secondary wall is common to *B. microphylla* and coniferous species. However, there is a slight difference; laccase activity was high in a broad range of S2 in differentiating reaction wood of *B. microphylla* (Figure 11 B: s). S2L in *B. microphylla* reaction wood has a mild gradient of lignin concentration in the S2 layer; the S2L region occupies a broad region of the S2 layer (Figure 11 C: mx). Thus, laccase activity coincides with the lignin distribution in the secondary wall in *Buxus* reaction wood.

Hemicellulose distribution in the cell wall of reaction wood

LM5, LM10, and LM22 antibodies label galactan [(1-4)-β-D-galactosyl residues], xylan [(1-4)-β-D-xylosyl residues of unsubstituted and relatively low-substituted xylans], and mannan

[β-linked mannan polysaccharides/β-(1→4)-manno-oligosaccharides], respectively.

LM5 labeling was weak around the compound middle lamella in normal wood fibers (Figure 12 B, D). This indicates that galactan is localized to the compound middle lamella in normal wood fibers. LM5 labeling was not detected in normal wood xylem of poplar (*Populus trichocarpa* Torr. & A. Gray × *P. koreana* Rehder) (Arend 2008), and was sparse in normal wood cell walls of willow (*Salix* spp.) (Gritsch 2015). In *P. radiata*, LM5 labeling was localized to the primary wall (around the compound middle lamella) (Donaldson and Knox 2012). Thus, our result coincides with that in conifer species. LM5 labeling was evident in the outer region of the S2 layer in reaction wood fibers in *B. microphylla* (Figure 12 A, C). This result indicates that galactan is localized to the outer region of the S2 layer in reaction wood fibers. Coniferous compression wood is rich in galactan, and is localized to the outer region of the S2 layer in the cell wall (Donaldson and Knox 2012, Kim et al. 2010). Tension wood is also rich in galactan, and is localized to the G layer (Arend 2008, Gritsch 2015). Although *Buxus* reaction wood also contains abundant galactan, like tension and compression woods, the distribution is similar to that in compression wood. Galactan is generally not localized to the secondary wall in woody angiosperms, but was detected in the secondary wall in *B. microphylla* reaction wood. This result suggests that galactan plays a key role in reaction wood. Moreover, this galactan distribution in the reaction wood cell wall is common to both *B. microphylla* and coniferous species. Thus, the function of galactan deposition is likely also common among them, and might be crucial for generating compressive growth stress.

LM10 labeling was localized to the entire secondary wall in normal wood fibers, and was abundant in the S1 layer (Figure 12 F, H). Xylan was localized to the entire secondary wall, and was abundant in the S1 layer. In poplar (Kim et al. 2012), *Zinnia elegans* (Northcote et al. 1989), and *Fagus crenata* (Awano et al 2002), xylan is localized to the secondary wall. Thus, xylan localization in *B. microphylla* normal wood is similar to that in other angiosperms. In contrast, in reaction wood fibers, LM10 labeling was localized to the S1 layer and inner region of the S2 layer, and was sparse in the outer region of S2 (Figure 12 F, H). Thus, xylan is localized to these regions in the reaction wood cell wall. In compression wood of *P. radiata*, xylan is localized to the compound middle lamella, S1 layer, and inner region of the S2 layer, but not the outer part of the S2 layer (Donaldson and Knox 2012). Xylan localization is common between *B. microphylla* and *P. radiata* in that the S2L region contains little xylan. This commonality suggests that the reduction in the xylan content in the outer region of the S2 layer might be involved in S2L formation. LM11, which also labels xylan, was used to

investigate xylan localization. The distribution of LM11 labeling was similar to that of LM10 (data not shown). Xylan in woody angiosperms is *O*-acetyl-4-*O*-methylglucuronoxylan; in the case of coniferous species, xylan is arabino-4-*O*-methylglucuronoxylans (Timell 1967). LM10 binds the former, and LM11 labels both the former and latter. The lack of a difference in the results of LM10 and LM11 labeling suggests that *B. microphylla* xylem likely does not contain arabino-4-*O*-methylglucuronoxylan, or that the two types of xylan have an identical localization.

LM22 labeling was localized to the S2 layer in normal and reaction woods. Xylem of woody angiosperms (hard wood) is mainly *O*-acetyl-4-*O*-methylglucuronoxylan with little glucomannan (Timell 1967); LM 22 labels glucomannan. Thus, glucomannan is likely localized to the S2 layer in normal and reaction woods. In reaction wood, however, labeling was slight in the central region of the S2 layer; LM22 labeling was slight on the inner side of S2L (Figure 12 I, K). The glucomannan content of compression wood is half that of normal wood (Nanayakkara et al. 2009). In *P. radiata*, the glucomannan content is lower in the outer portion of S2 in compression wood than in normal wood (Donaldson and Knox 2012). The reduction in the amount of glucomannan in *B. microphylla* reaction wood is similar to that in compression wood, but the distribution in the cell wall is different. LM21, which also labels mannan, was used to investigate mannan localization. The distribution of LM21 labeling was similar to that of LM22 (data not shown). Donaldson and Knox (2012) reported that LM21 and 22 labeled lignified cells within *P. radiata* xylem, but the labeling was localized to relatively low lignification regions; e.g., the secondary wall of normal wood and inner portion of S2 of compression wood. Based on this result, the authors assumed that glucomannan functions in limiting lignification. The localization of glucomannan did not coincide with the S2L region. Thus, the function of mannan in *B. microphylla* reaction wood may be slightly different from that in compression wood.

General discussion

Common points among *B. microphylla* and coniferous species: In this study, I investigated the factors involved in the increased lignin content in *B. microphylla* reaction wood; e.g., expression of genes involved in lignin synthesis, laccase activity localization, and hemicellulose distribution in the cell wall. The majority of the results indicated commonalities between *B. microphylla* reaction wood and compression wood. These findings suggest that lignification in *B. microphylla* reaction wood is basically identical to that in coniferous compression wood.

Development of reaction woods during plant evolution: *Buxus* reaction wood resembles coniferous compression wood in anatomy and functionality, likely due to convergent evolution. However, the factors involved in the increased lignin content are almost identical, which cannot be explained by convergent evolution. Thus, development of *Buxus* reaction wood also cannot be explained by this theory. Rather than convergent evolution, our findings suggest that *Buxus* reaction wood has a common origin with compression wood. The genus *Buxus* is classified as a eudicot, and many woody species included in this clade form typical tension wood. Therefore, I assume that after angiosperms diverged from gymnosperms, the ancestor of *Buxus* might have had a latent ability to produce compression wood, which was subsequently re-expressed due to unknown factors.

Compressive growth stress and generation of *Buxus* reaction wood: *Buxus* reaction wood generates compressive growth stress (Bailleres et al. 1949). The lignin swelling hypothesis (Boyd 1972) suggests that this stress is due to the combination of a large microfibril angle and high lignin content. Yamamoto *et al*. (1991) reported that microfibril angle and lignin content are correlated with compressive growth stress in coniferous species. Moreover, Okuyama *et al*. (1998) confirmed that the lignin concentration in S2L is correlated positively with compressive growth stress. The lignin swelling hypothesis is applicable to *Buxus* reaction wood because it has an elevated lignin content in the secondary wall and a large microfibril angle (Yoshizawa et al. 1993). Our results suggest that the lignification process in *B. microphylla* reaction wood is basically identical to that in compression wood. Thus, the mechanism of generation of compressive growth stress might be identical between the two types of wood.

Table 4. Primer pairs used for qRT-PCR

Gene name	Forward primer (5'→3')	Reverse primer (5'→3')	Product size
BmTIF	AAGGAATTCTGCTGCAATGG	ACAATTCCAGCCTGCACAAG	116 bp
BmPAL1	ATCCCTGCAGTGGCACTTAC	ATGCAATTCTCGCACTCTCC	180 bp
BmCAD1	GTGACGGTTTACAGCCCACT	GACCCAGAATTCCTCCTCTCA	70 bp
BmLac1	CGCTTTAGCAGCTCAACTCC	GCTTTGGCAGTTCTTCTTGG	181 bp
BmLac2	CGTCTTCCACTCTTCAAACCAAC	CTTGGCAGGTTTGGTTCACTG	190 bp
BmLac3	CAGCCATTACTCTCACCAACAC	AACAACACGGCTGCCATTAG	194 bp
BmLac4	ATCGTCCCATTCCTCTTCCT	TGAAGAAGAAACGCCTGTCC	182 bp
BmLac5	CAAGAACGGCGTGTCCATA	GTGTTACCTGGTGGGCAGTT	183 bp

Table 5. Similarity of cloned *B. microphylla* genes to genes in the *Arabidopsis thaliana* genome

Gene name	Accession	Identity	E-value	Most similar gene	Locus
BmTIF	AB762681	93%	5E–45	Translation initiation factor SUI1 family protein	AT1G54290
BmPAL	AB762676	78%	6E–70	PAL2	AT3G53260
BmCAD	AB762677	71%	E–44	CAD4	AT3G19450
BmLac1	AB762671	64%	E–132	Laccase 6	AT2G46570
BmLac2	AB762672	69%	E–143	Laccase 17	AT5G60020
BmLac3	AB762673	69%	E–134	IRX12, LAC4	AT2G38080
BmLac4	AB762674	71%	E–144	Laccase 17	AT5G60020
BmLac5	AB762675	67%	E–134	Laccase 5	AT2G40370

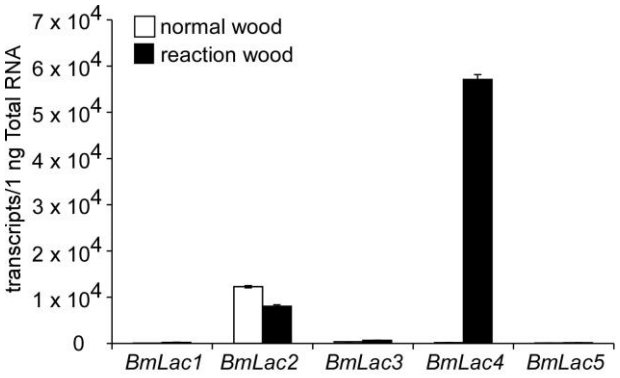

Figure 9. Expression of five laccase genes in differentiating xylem. Transcript abundance is the copy number of the tested gene per 1 ng of total RNA. Values are means ± SD of three independent measurements for each gene.

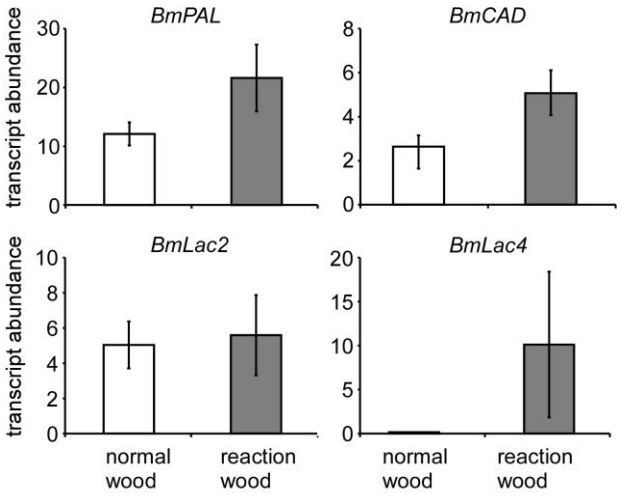

Figure 10. PAL, CAD, and laccase expression in differentiating xylem. Transcript abundance is the ratio of the copy number of the tested gene to that of a reference gene (*BmTIF*). Values are means ± SD of four biological replicates for each gene.

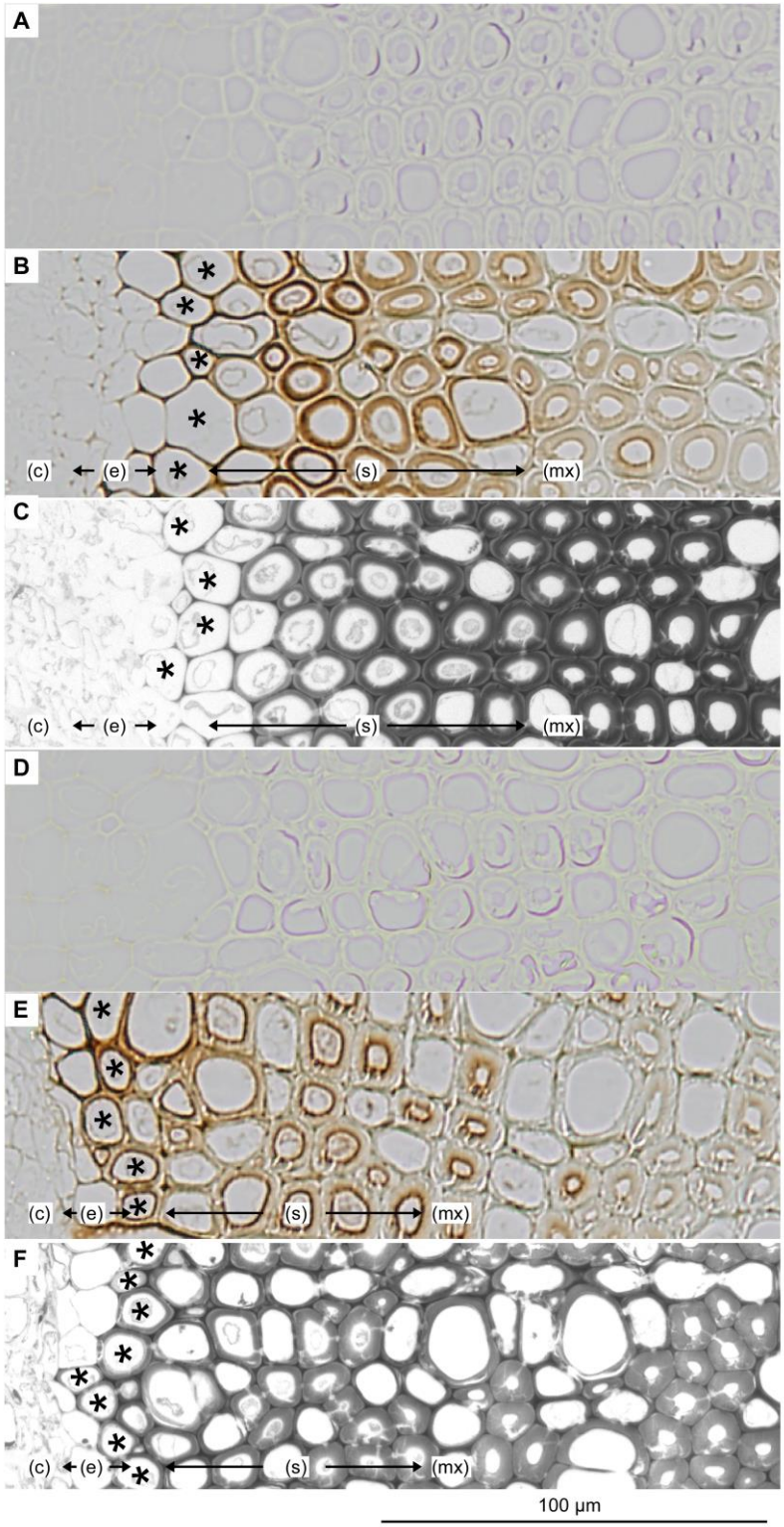

Figure 11. Localization of laccase activity and lignin deposition in differentiating xylem, and their relationship. A) Reaction wood section autoclaved and stained for laccase activity. B) Reaction wood section stained for laccase activity. C) Lignin deposition in differentiating reaction wood section. D)

Normal wood section autoclaved and stained for laccase activity. E) Normal wood section stained for laccase activity. F) Lignin deposition in a differentiating normal wood section. In each image, the cambium is on the left, and the pith on the right. Asterisks indicate cells that have begun secondary wall thickening (confirmed by polarizing microscopy; Fujita et al. 1978, Takabe et al. 1981). (c) cambial zone; (e) expansion zone, cells before onset of secondary wall thickening; (s) cells during secondary wall formation; (mx) mature cells.

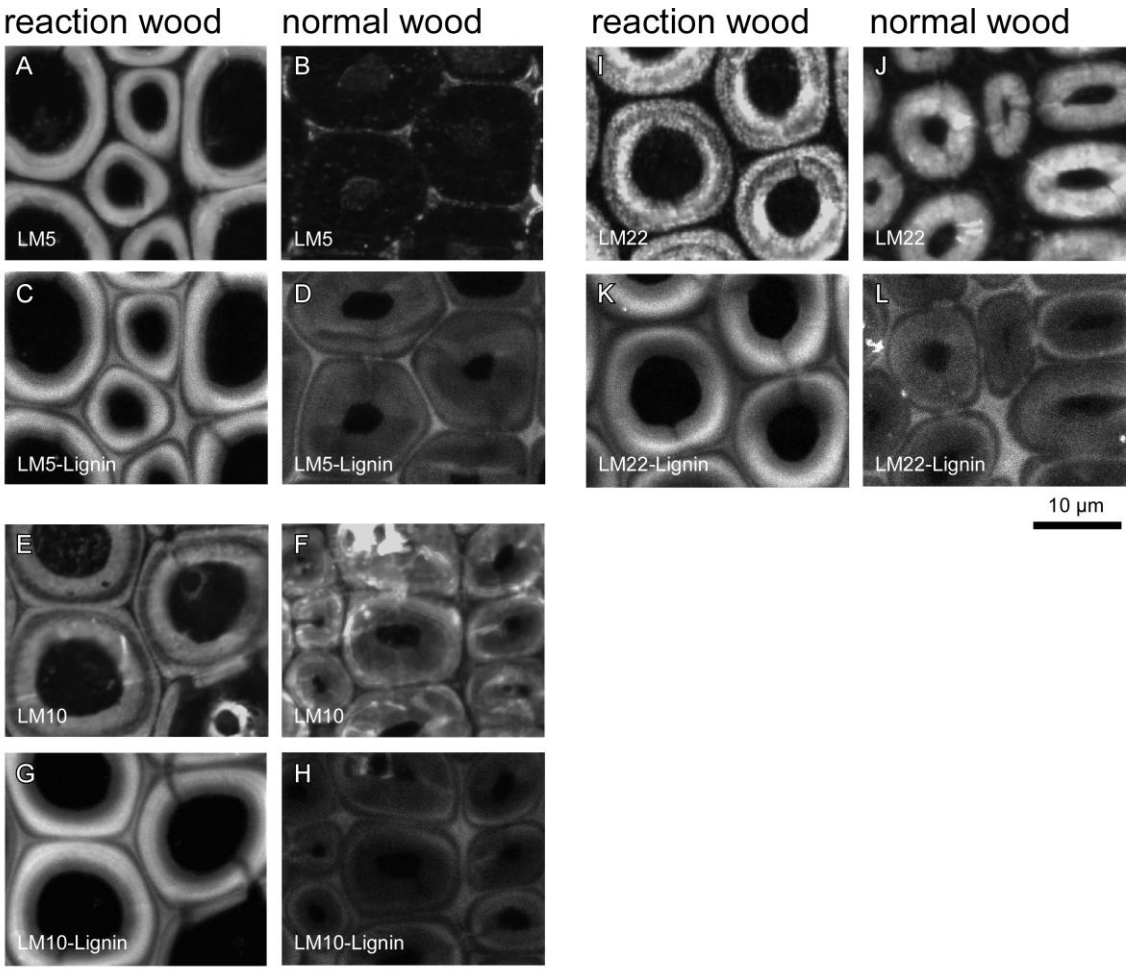

Figure 12. Immunolocalization of hemicelluloses in mature xylem.

A, B) LM5 labeling in reaction and normal woods. C, D) Lignin distribution in A and B.

E, F) LM10 labeling in reaction and normal woods. G, H) Lignin distribution in E and F.

I, J) LM22 labeling in reaction and normal woods. K, L) Lignin distribution in I and J.

Chapter 5 Conclusions

In the present study, we found a laccase gene would be involved in lignification of compression wood cell wall, and we investigated the laccase (CoLac1) function. *In situ* assay on CoLac1 laccase localization was performed and the function was discussed. In addition, we assessed *Buxus* compression wood to discuss generality of our results. The statements below summarize my findings.

1. Differentiating compression wood tracheids upregulate almost all enzymes involved in lignin synthesis to increase monolignol supply.
2. Differentiating compression wood tracheids express Colac1 laccase to promote monolignol oxidization (lignin deposition), which lead to increase of lignin content in the cell wall.
3. Differentiating compression wood tracheids secret CoLac1 laccase to cell wall and localize it in S2L region, where laccase activity become high, resulting in high lignin concentration in this region. That is, CoLac1 laccase lead to S2L formation.
4. *Buxus microphylla* var. japonica, which is included clade of care eudicot, have many common points in compression wood lignification: [1] differentiating compression wood fibers specifically express a laccase gene (*BmLac4*); [2] increase laccase activity in the secondary wall, and the localization coincide with lignin distribution; [3] and localized galactan in the outer portion of S2 layer. These might be potential essential factors in lignification of compression wood and generation of compressive growth stress.

Our knowledge on compression wood differentiation had been limited in prediction supported by information on gene expression. That is, demonstrating upregulation of a laccase gene suggested no more than an involvement of laccase. Thus experimental evidence has been needed to discuss laccase function. In the present study, using histochemical technique, we experimentally reveal localization of laccase activity and CoLac1 protein. This result strongly support laccase (CoLac1 laccase in *Chamaecyparis obtusa*) is a factor in S2L formation. To obtain strong evidence on the function, a tree in which compression-wood-specific laccase is down-regulated must be investigated.

Acknowledgements

I am grateful to Associate Professor Matato Yoshida, Professor Hiroyuki Yamamoto, and Doctor Saori Sato for their instructions and encouragements during this study. I also thank Proffessor Kazuhiko Fukushima, Doctor Miyuki Matsuo, and students of my laboratory for helpful discussion and suggestions.

References

[1] Adler E (1977) Lignin chemistry—past, present and future. *Wood Science Technology* 11, 169-218.

[2] Aiso H, Hiraiwa T, Ishiguri F, Iizuka K, Yokota S, Yoshizawa N (2013) Anatomy and lignin distribution of "compression-wood-like reaction wood" in Gardenia jasminoides. I*AWA JOURNAL* 34, 263-272.

[3] Aiso H, Ishiguri F, Takashima Y, Iizuka K, Yokota S (2014) Reaction wood anatomy in a vessel-less angiosperm Sercandra glabra. *IAWA JOURNAL* 35, 116-126.

[4] Allona I, Quinn M, Shoop E, Swope K, St Cyr S, Carlis J, Riedl J, Retzel E, Campbell MM, Sederoff R, Whetten RW (1998) Analysis of xylem formation in pine by cDNA sequencing. *Proceedings of the National Academy of Sciences of the United States of America* 95, 9693–9698.

[5] Altaner CM, Tokareva EN, Jarvis MC, Harris PJ (2010) Distribution of (1 -> 4)-beta-galactans, arabinogalactan proteins, xylans and (1 -> 3)-beta-glucans in tracheid cell walls of softwoods. *Tree physiology* 30, 782-793.

[6] Arend M (2008) Immunolocalization of (1,4)-beta-galactan in tension wood fibers of poplar. *Tree Physiology* 28, 1263-1267.

[7] Awano T, Takabe K., Fujita M (2002) Xylan deposition on secondary wall of Fagus crenata fiber. *Protoplasma* 219, 106 -115.

[8] Bao W, O'malley DM, Whetten R, Sederoff RR (1993) A laccase associated with lignification in loblolly pine xylem. *Science* 260, 672–674.

[9] Bailleres H, Castan M, Monties B, Pollet B, Lapierre, C (1997) Lignin structure in *Buxus sempervirens* reaction wood. *Phytochemistry* 44, 35-39.

[10] Barros J, Serk H, Granlund I, Pesquet E (2015) The cell biology of lignification in higher plants. *Annals of botany* 115, 1053-1074.

[11] Berthet S, Demont-Caulet N, Pollet B, Bidzinski P, Ce´zard L, Le Bris P, Borrega N, Herve´ J, Blondet E, Balzergue S, Lapierre C, Jouanin L (2011) Disruption of LACCASE4 and 17 results in tissue-specific alterations to lignification of Arabidopsis thaliana stems. *Plant Cell* 23, 1124–1137.

[12] Boerjan W, Ralph J, Baucher M (2003) Lignin biosynthesis. *Annual Review of Plant Biology* 54, 519–546.

[13] Boyd JD (1972) Tree growth stresses. V. Evidence of an origin in differentiation and lignification. *Wood science and technology* 6, 251-262.

[14] Cosio C, Dunand C (2009) Specific functions of individual class III peroxidase genes. *Journal of experimental botany* 60, 391–408.

[15] Donaldson LA (2001) Lignification and lignin topochemistry - an ultrastructural view. *Phytochemistry* 57, 859-873.

[16] Donaldson LA, Knox JP (2012) Localisation of cell wall polysaccharides in normal and compression wood of radiata pine: relationships with lignifications and microfibril orientation. *Plant Physiology* 158, 642–653.

[17] Fagerstedt KV, Kukkola EM, Koistinen VVT, Takahashi J, Marjamaa K (2010) Cell all lignin is polymerised by class III secretable plant peroxidases in Norway spruce. *Journal of integrative plant biology* 52, 186-194.

[18] Fujita M, Saiki H, Harada H (1978) The secondary wall formation of compression wood tracheids. II. Cell wall thickening and lignification. *Mokuzai Gakkaishi* 24, 158-163.

[19] Fergus BJ, Procter AR., Scott JAN, Goring DAI (1969) The distribution of lignin in spruce wood as determined by ultraviolet microscopy. *Wood Science Technology* 3, 117–138.

[20] Gritsch (2015) G-fibre cell wall development in willow stems during tension wood induction. *Journal of Experiment of Botany* 66, 6447-6459.

[21] Kim JS, Awano T, Yoshinaga A, Takabe, K (2010) Immunolocalization of beta-1-4-galactan and its relationship with lignin distribution in developing compression wood of Cryptomeria

japonica. *Planta* 232,109–119.

[22] Kim JS, Daniel G (2012) Distribution of glucomannans and xylans in poplar xylem and their changes under tension stress. *Planta* 236, 35–50.

[23] Kojima, M., Becker, V.K., Altaner, C.M (2012) An unusual form of reaction wood in Koromiko [Hebe salicifolia G. Forst. (Pennell)], a southern hemisphere angiosperm. *Planta* 235, 289-297.

[24] Koutaniemi S, Warinowski T, Kärkönen A, Alatalo E, Fossdal CG, Saranpää P, Laakso T, Fagerstedt KV, Simola LK, Paulin L, Rudd S, Teeri TH (2007) Expression profiling of the lignin biosynthetic pathway in norway spruce using EST sequencing and real-time RT-PCR. Plant Molecular Biology 65, 311-328.

[25] Marjamaa K, Hildén K, Kukkola E, Lehtonen M, Holkeri H, Haapaniemi P, Koutaniemi S, Teeri TH, Fagerstedt K, Lundell T (2006) Cloning, characterization and localization of three novel class III peroxidases in lignifying xylem of norway spruce (Picea abies). *Plant Molecular Biology* 61, 719–732.

[26] McCaig BC, Meagher RB, Dean JFD (2005) Gene structure and molecular analysis of the laccase-like multicopper oxidase (LMCO) gene family in *Arabidopsis thaliana*. *Planta* 221, 619-636.

[27] McDougall GJ (2000) A comparison of proteins from the developing xylem of compression and non-compression wood of branches of sitka spruce (Picea sitchensis) reveals a differentially expressed laccase. *Journal of Experiment of Botany* 51, 1395–1401.

[28] Nanayakkara B, Manley-Harris M, Suckling, ID, Donaldson LA. (2009) Quantitative chemical indicators to assess the gradation of compression wood. *Holzforschung* 63, 431–439.

[29] Nimz HH, Robert D, Faix O, Nemr M (1981) Carbon-13 NMR Spectra of Lignins, 8 Structural differences between lignins of hardwoods, softwoods, grasses and compression wood. *Holzforschung* 35, 16-26.

[30] Northcote DH, Davey R, Lay J. (1989) Use of antisera to localize callose, xylan and arabinogalactan in the cell-plate, primary and secondary walls of plant cells. *Planta* 178, 353-366.

[31] Okuyama T, Yamamoto H, Iguchi M, Yoshida M. (1990) Generation process of growth stresses in cell walls. II. Growth stress in tension wood, *Mokuai Gakkaishi* 36, 797-803

[32] Okuyama T, Yamamoto H, Yoshida M. Hattori Y, Archer RR. (1994) Growth stress in wood-Role of microfibrils and lignification. *Annals des sciences forestieres* 51, 291-300

[33] Okuyama T, Takeda H, Yamamoto H Yoshida M. 1998. Relation between growth stress and lignin concentration in the cell wall. *Journal of Wood Science* 44, 83-89.

[34] Onaka F. (1949) Studies on compression- and tension-wood. *Wood Research* 1, 1-88.

[35] Page RD (1996) TreeView: an application to display phylogenetic trees on personal computers. *Computer Applications in the Biosciences* 12, 357–358.

[36] Ranocha P, McDougall G, Hawkins S, Sterjiades R, Borderies G, Stewart, D, Cabanes-Macheteau M, Boudet AM, Goffner D (1999) Biochemical characterization, molecular cloning and expression of laccases—a divergent gene family—in poplar. *European Journal of Biochemistry* 259, 485–495.

[37] Sato Y, Bao W, Sederoff R, Whetten R (2001) Molecular cloning and expression of eight laccase cDNAs in loblolly pine (Pinus taeda). *Journal of Plant Research* 114, 147–155.

[38] Scurfield G. (1973) Reaction wood: its structure and function. *Science* 179, 647–655.

[39] Shigeto J, ItohY, Tsutsumi Y, Kondo R (2012) Identification of Tyr74 and Tyr177 as substrate oxidation sites in cationic cell wall-bound peroxidase from *Populus alba* L. *FEBS Journal* 279, 348-357.

[40] Shigeto J, Kiyonaga Y, Fujita K, Kondo R, Tsutsumi Y (2013) Putative cationic cell-wall-bound peroxidase homologues in Arabidopsis, AtPrx2, AtPrx25, and AtPrx71, are involved in lignification. *Journal of agricultural and food chemistry* 61, 3781-3788.

[41] Shigeto J, Nagano M, Fujita K, Tsutsumi Y (2014) Catalytic profile of Arabidopsis peroxidases, AtPrx-2, 25 and 71, contributing to stem lignification. *PLoS ONE* 9, e105332.

[42] Shigeto J, Itoh Y, Hirao S, Ohira K, Fujita K, Tsutsumi Y (2015) Simultaneously disrupting AtPrx2, AtPrx25 and AtPrx71 alters lignin content and structure in Arabidopsis stem. *Journal of integrative plant biology* 57, 349-356.

[43] Sterjiades R, Dean JFD, Eriksson K L (1992) Laccase from sycamore maple (Acer pseudoplatanus) polymerizes monolignols. *Plant Physiology* 99, 1162–1168.

[44] Takabe K, Fujita M, Harada H, Saiki H (1981) Lignification process of Japanese black pine (*Pinus thunbergii* Parl.) tracheids. *Mokuzai Gakkaishi* 27, 813-820.

[45] Terashima, N (1989) An improved radiotracer method for studying formation and structure of lignin. In Lewis NG, Paice MG, eds, Plant Cell Wall Polymers, Biogenesis and Biodegradation, ACS Symposium.Series, vol.399. Am Chem Soc, Washington, pp 148-159.

[46] Terashima N, Fukushima K, He LF, Takabe K (1993) Comprehensive model of the lignified plant cell wall. In Jung HG, Buxton DR, Hatfield RD, Ralph J, eds, Forage Cell Wall Structure and Digestibility, Am Soc Agr, Madison, pp 247-270.

[47] Timell TE (1967) Recent progress in the chemistry of wood hemicelluloses. *Wood Science and Technology* 1, 45-70.

[48] Timell, TE (1986) Compression wood in gymnosperms, vol 1. Springer, Berlin.

[49] Vandesompele J, De Preter K, Pattyn,F, Poppe B, Van Roy N, De Paepe A, Speleman F (2002) Accurate normalization of real-timequantitative RT-PCR data by geometric averaging of multiple internal control genes. *Genome Biology* 3:research 0034.1.

[50] Vanholme R, Demedts B, Morreel K, Ralph J, Boerjan, W (2010) Lignin biosynthesis and structure. *Plant Physiol* 153, 895–905.

[51] Villalobos DP, Díaz-Moreno SM, Said E-S S, Cañas RA, Osuna D, Van Kerckhoven S HE, Bautista R, Claros MG, Canovas FM, Canton, FR (2012) Reprogramming of gene expression during compression wood formation in pine: coordinated modulation of S-adenosylmethionine,

lignin and lignan related genes. *BMC Plant Biology* 12, 100–116.

[52] Whetten R, Sun Y H, Zhang Y, Sederoff R (2001) Functional genomics and cell wall synthesis in loblolly pine. *Plant Molecular Biology* 47, 275–291.

[53] Wilson BF, Archer RR (1977) Reaction wood: induction and mechanical action. *Annual Review of Plant Physiology* 28, 23–43.

[54] Yamamoto H, Okuyama T, Yoshida M, Sugiyama K (1991) Generation process of growth stresses in cell walls. III. Growth stress in compression wood. *Mokuzai Gakkaishi* 37, 94–100.

[55] Yamamoto, H. 1998. Generation mechanism of growth stresses in wood cell walls: Roles of lignin deposition and cellulose microfibril during cell wall maturation. *Wood Science and Technology* 32, 171-182.

[56] Yamamoto H, Yoshida M, Okuyama T (2002) Growth stress controls negative gravitropism in woody plant stems. *Planta* 216, 280–292.

[57] Yamashita S, Yoshida M, Takayama S, Okuyama T (2007) Stem-righting mechanism in gymnosperm trees deduced from limitations in compression wood development. *Annals of Botany* 99, 487-493.

[58] Yamashita S, Yoshida M, Yamamoto H, Okuyama, T (2008) Screening genes that change expression during compression wood formation in Chamaecyparis obtusa. *Tree Physiology* 28, 1331–1340.

[59] Yamashita S, Yoshida M, Yamamoto H (2009) Relationship between development of compression wood and gene expression. *Plant Science* 176, 729–735.

[60] Yoshida M, Ohta H, Yamamoto H, Okuyama T (2002) Tensile growth stress and lignin distribution in the cell walls of yellow poplar, Liriodendron tulipifera Linn. *Trees* 16, 457–464.

[61] Yoshinaga A, Kusumoto H, Laurans F, Pilate G, Takabe K (2012) Lignification in poplar tension wood lignified cell wall layers. *Tree physiology* 32, 1129-1136.

[62] Yoshizawa N, Satoh M, Yokota S, Idei T (1993) Formation and structure of reaction wood in *Buxus microphylla* var. insularis Nakai. *Wood Science and Technology* 27, 1-10.

[63] Zhao Q, Nakashima J, Chen F, Yin YB, Fu CX, Yun JF, Shao H, Wang XQ, Wang ZY, Dixon RA (2013) LACCASE is necessary and nonredundant with PEROXIDASE for lignin polymerization during vascular development in Arabidopsis. *Plant Cell* 25, 3976–3987.